THE MULTI-COMPONENT REACTIVE TRANSPORT MODULE

CW2D

FOR CONSTRUCTED WETLANDS

FOR THE HYDRUS SOFTWARE PACKAGE

Manual - Version 1.0

by

Günter Langergraber[1] and Jirka Šimůnek[2]

March 2006

[1] Institute for Sanitary Engineering and Water Pollution Control
BOKU - University of Natural Resources and Applied Life Sciences, Vienna
Muthgasse 18, A-1190 Vienna, Austria

[2] Department of Environmental Sciences
University of California Riverside
Riverside, CA, 92521, USA

Abstract

Langergraber, G. and J. Šimůnek, The Multi-Component Reactive Transport Module CW2D for Constructed Wetlands for the HYDRUS Software Package, *Hydrus Software Series 2*, Department of Environmental Sciences, University of California Riverside, Riverside, California, USA, p. 72, 2006.

Constructed wetlands are becoming increasingly popular worldwide for removing nutrients, organics, trace elements, pathogens, or other pollutants from wastewater and/or runoff water. This manual describes a multi-component reactive transport module CW2D (**C**onstructed **W**etlands **2D**, Langergraber, 2001, Langergraber and Šimůnek, 2005), that was developed as an extension of the HYDRUS-2D variably-saturated water flow and solute transport program (Šimůnek et al., 1999). CW2D was developed to model the biochemical transformation and degradation processes in subsurface-flow constructed wetlands. The biochemical degradation and transformation processes for organic matter, nitrogen and phosphorus are described. The mathematical structure of CW2D is based on the IWA Activated Sludge Models (Henze et al., 2000). Monod-type expressions are used to describe the process rates. All process rates and diffusion coefficients are temperature dependent. The biochemical components defined in CW2D include dissolved oxygen, three fractions of organic matter (readily- and slowly-biodegradable, and inert), four nitrogen compounds (ammonium, nitrite, nitrate, and dinitrogen), inorganic phosphorus, and heterotrophic and autotrophic micro-organisms. Organic nitrogen and organic phosphorus are modelled as part of the COD. Heterotrophic bacteria are assumed to be responsible for hydrolysis, mineralization of organic matter (aerobic growth) and denitrification (anoxic growth). Autotrophic bacteria are assumed to be responsible for nitrification, which is modelled as a two-step process. All micro-organisms are assumed to be immobile. Lysis is considered to be the sum of all decay and loss processes.

The manual provides a short overview of the constructed wetland technology, describes internal details of the reactive transport CW2D module, its main principles, its mathematical formulations, and a set of default parameters based on the literature review. It also describes how CW2D is implemented into HYDRUS (Šimůnek et al., 2006a, 2006b), what modifications were made in the original code, and how the new module can be run using the HYDRUS graphical user interface. Finally, it presents several illustrative and verification examples of the use of CW2D, and description of additional new input and output files.

DISCLAIMER

This report documents version 1.0 of the implementation of the CW2D module into the HYDRUS graphical user interface. The CW2D module was developed as a supplemental module of the HYDRUS software package, to model the biochemical transformation and degradation processes in subsurface flow constructed wetlands. The software has been verified against selected test cases. However, no warranty is given that the program is completely error-free. If you do encounter problems with the code, find errors, or have suggestions for improvement, please contact one of the authors at

Günter Langergraber
Tel: +43-(0)1-36006-5814
Fax: +43-(0)1-368 99 49
email: guenter.langergraber@boku.ac.at

Jirka Šimůnek
Tel: 1-951-827-7854
Fax: 1-951-787-3993
E-mail: jiri.simunek@ucr.edu

Table of contents

List of Figures

List of Tables

1 Introduction

Constructed wetlands (CWs) are engineering structures designed to improve water quality. Wetlands involve a complex mixture of water, substrate, plants, litter, and a variety of micro-organisms to provide optimal conditions for improving water quality. They are effective in removing organic matter, nitrogen, phosphorus, and also in decreasing the concentrations of heavy metals, organic chemicals, and pathogens from wastewater and/or runoff water. Understanding of constructed wetlands function is made difficult by the large number of physical, chemical, and biological processes, that are all active at the same time and that mutually influence each other. Numerical simulators can represent invaluable tools for analysing, studying, and improving understandings of complex systems such as constructed wetlands.

This manual describes the multi-component reactive transport module CW2D (**C**onstructed **W**etlands **2D**, Langergraber, 2001, Langergraber and Šimůnek, 2005), which was developed as an extension of the HYDRUS-2D variably-saturated water flow and solute transport program (Šimůnek et al., 1999) to model the biochemical transformation and degradation processes in subsurface flow constructed wetlands. The biochemical degradation and transformation processes for organic matter, nitrogen and phosphorus are described. The mathematical structure of CW2D is based on the IWA Activated Sludge Models (Henze et al., 2000). Monod-type expressions are used to describe the process rates. All process rates and diffusion coefficients are assumed to be temperature dependent. The biochemical components defined in CW2D include dissolved oxygen, three fractions of organic matter (readily- and slowly-biodegradable, and inert), four nitrogen compounds (ammonium, nitrite, nitrate, and dinitrogen), inorganic phosphorus, and heterotrophic and autotrophic micro-organisms. Organic nitrogen and organic phosphorus are modelled as part of the COD. Heterotrophic bacteria are assumed to be responsible for hydrolysis, mineralization of organic matter (aerobic growth) and denitrification (anoxic growth). Autotrophic bacteria are considered to be responsible for nitrification, which is modelled as a two-step process. All micro-organisms are assumed to be immobile. Lysis is considered to represent the sum of all decay and sink processes.

Chapter 2 provides a short overview of the constructed wetland technology. Chapter 3 describes internal details of the reactive transport CW2D module, its main principles, its mathematical formulations, and a set of default parameters based on the literature review. Chapter 4 describes how CW2D is implemented into HYDRUS, what modifications were made in the original code, and how the new module can be run using the HYDRUS graphical user interface (Šimůnek et al., 2006a). Chapter 5 provides several illustrative and verification examples of the use of CW2D. Finally, description of additional new input and output files is given in Chapters 6 and 7, respectively.

2 Constructed wetland technology

Constructed wetlands (CWs) or wetland treatment systems are wetlands designed to improve water quality. Such wetlands involve a complex mixture of water, substrate, plants, litter (fallen plant material), and a variety of micro-organisms (most importantly bacteria) to provide the treatment conditions for improvement of water quality found in natural wetlands, but have the flexibility of being constructed and thus their various functions can be optimized as needed. For an optimal support of different treatment mechanisms, various types of CWs optimised for different applications can be used (Kadlec and Knight, 1996).

CWs are used worldwide to treat water of different qualities (Kadlec et al., 2000; Langergraber and Haberl, 2001; Haberl et al., 2003). The experience shows that CWs can be used successfully with different quality of the influent water and under various climatic conditions. They are effective in removing organic matter, nitrogen, phosphorus, and additionally for decreasing the concentrations of toxic trace metals, organic chemicals, and pathogens.

In general the use of CWs provides a relatively simple, inexpensive, and robust solution for the treatment of water. Compared to other treatment options, CWs usually need lower operational and maintenance expenses. Additional benefits include CWs tolerance to fluctuations in fluxes and pollution loads, their facilitation of water reuse and recycling, creation of habitat for many wetland organisms, and the more aesthetic appearance of natural systems compared to technical treatment options (Kadlec at al., 2000).

Constructed wetlands include the surface flow (SF) and subsurface flow (SSF) CWs (Kadlec and Knight, 1996). Surface flow constructed wetlands are generally densely vegetated by a variety of plant species and typically have water depths of less than 0.4 m. Open water areas can be incorporated into an overall design to optimise hydraulic operations with wildlife habitat enhancements. Typical hydraulic loading rates are between 0.7 and 5.0 $cm.d^{-1}$ (between 2 and 14 ha per 1000 m^3 per day) in constructed surface flow treatment wetlands. Subsurface flow wetland technology is based on the work of Seidel (1967). Since then the technology has become increasingly popular in many European countries and is nowadays applied worldwide (Vymazal et al., 1998; Kadlec at al., 2000). Surface flow constructed wetlands use a bed of soil or gravel as a substrate for the growth of rooted emergent wetland plants. Mechanically pre-treated wastewater flows by gravity horizontally or vertically through the bed substrate, where it contacts a mixture of facultative microbes living in association with the substrate and plant roots.

Subsurface vertical flow constructed wetlands (SSVF CWs) with intermittent feeding are used widely today due to their good efficiency regarding the removal of ammonium nitrogen. Although much experience exists in constructing and operating such systems, their design is still based mostly on empirical rules, such as requiring a specific area per person or using simple first-order kinetic rates. However, Kadlec (2000) concluded that first-order models are inadequate for the design of treatment wetlands, especially SSF CWs.

The main reason for developing a simulation tool that describes complex processes in subsurface flow constructed wetlands was to create a computational tool for analyzing, evaluating, and improving our understanding of various mutually-dependent interactions within the black box "constructed wetland". Once the simulation tool provides reliable

description of processes in SSF CWs, the existing design criteria can be verified and finally the design of constructed wetlands can be optimised (Langergraber, 2003).

3 The CW2D multi-component reactive transport module

3.1 Background

The need for a numerical model describing biochemical transformation and degradation processes in subsurface flow constructed wetlands motivated the development of the multi-component reactive transport module CW2D (Langergraber, 2001) for incorporation into the HYDRUS-2D variably-saturated water flow and solute transport program. CW2D is able to model the biochemical transformation and degradation processes for organic matter, nitrogen and phosphorus. The CW2D module considers 12 components and 9 processes. The components include dissolved oxygen, organic matter (three fractions of different degradability), ammonium, nitrite, nitrate, and dinitrogen nitrogen, inorganic phosphorus, and heterotrophic and autotrophic micro-organisms. Organic nitrogen and organic phosphorus are modelled as nutrient contents of the organic matter. The processes considered are hydrolysis, mineralization of organic matter, nitrification (which is modelled as a two-step process), denitrification, and a lysis process for the micro-organisms.

The mathematical structure of CW2D is based on the mathematical structure of the Activated Sludge Models introduced by Henze et al. (2000). The Activated Sludge Model No. 1 (ASM1) by Henze et al. (1985) was developed to describe organic matter and nitrogen removal in activated sludge plants. ASM1 became very popular and is nowadays the standard model for simulating activated sludge processes. A lot of extensions and sub-models of ASM1 exist that significantly extent its applicability. Further developments led to the incorporation of phosphorus removal into the Activated Sludge Model (ASM2 by Henze et al., 1995). ASM2 had several limitations that were partly corrected and overcome in ASM2D (Henze et al., 1999). In the latest version, ASM3 (Gujer et al., 1999), the lysis process was replaced with a respiration process.

Major assumptions in all Activated Sludge Models are (a) a constant value of pH, (b) constant coefficients in the rate equations, and (c) constant stoichiometric factors. The various ASM models are valid only for domestic wastewater and are applicable within the temperature range of 10 to 25°C (Henze et al., 2000). Activated Sludge Models assume that nitrification occurs in one step, i.e., that ammonium is directly converted (nitrified) into nitrate. The two-step nitrification model used in CW2D (i.e., sequential nitrification of ammonium into nitrite and nitrate) is based on models presented by Nowak (1996) and Brouwer et al. (1998).

Activated sludge plants are usually modelled as a number of homogeneous, completely stirred reactors that are organized in series or parallel. Several papers (e.g., Makina and Wells, 2000a, 2000b) addressed the non-ideal hydraulic behaviour of activated sludge reactors. In their model, solute transport is described using advection-dispersion equation that is coupled with a reactive model, such as the Activated Sludge Model. The same principle for coupling the general governing transport equations with the reactive model was used in CW2D. Due to its implementation in HYDRUS-2D, CW2D additionally also considers the transient variably-saturated water flow described with the Richards equation.

3.2 Description of CW2D

The multi-component reactive transport module CW2D is able to model the biochemical elimination processes for carbon, nitrogen and phosphorus. The module considers 12 components and 9 processes. The **components** defined in CW2D include:

- **dissolved oxygen**, O_2 [mg_{O2}/l],
- organic matter [mg_{COD}/l] (three pools of organic matter (OM) expressed in units of chemical oxygen demand (COD) are considered: **readily** and **slowly biodegradable**, and **inert organic matter**; CR, CS, and CI, respectively),
- nitrogen [mg_N/l] (**ammonium** nitrogen NH_4^+, **nitrite** nitrogen NO_2^-, **nitrate** nitrogen NO_3^-, and **dinitrogen** nitrogen N_2),
- **inorganic phosphorus**, IP [mg_P/l],
- **heterotrophic micro-organisms**, XH [mg_{COD}/l],
- autotrophic micro-organisms (**Nitrosomonas** XANs and **Nitrobacter** XANb) [mg_{COD}/l].

Organic nitrogen and organic phosphorus are modelled as nitrogen and phosphorus content of the COD (chemical oxygen demand). It is assumed that the organic matter is present only in the aqueous phase and that all reactions occur only in the aqueous phase as well ($rs_j = 0$). Adsorption is considered for ammonium nitrogen (NH_4^+), and inorganic phosphorus (IP). Adsorption is assumed to be a kinetic process.

Biofilms in CW2D are assumed to be ideal, composed of a homogeneous matrix of micro-organisms with all species uniformly distributed over the biofilms. All micro-organisms are assumed to be immobile and hence were associated exclusively with the solid phase. Lysis represents the sum of all decay and loss processes of all micro-organisms involved, with the rate of lysis being independent of environmental conditions.

In CW2D it is assumed that **heterotrophic bacteria** include all bacteria that are responsible for hydrolysis, mineralization of organic matter (aerobic growth) and denitrification (anoxic growth).

- **Hydrolysis.** Hydrolysis describes the conversion of slowly into readily biodegradable organic matter (COD), with a small fraction being converted into inert COD. Ammonium (NH_4^+) and orthophosphate (IP) are released during this transformation process. It is further assumed that hydrolysis takes place independently of the oxygen conditions.
- **Aerobic growth of heterotrophic bacteria.** This process consumes oxygen (O_2) and readily biodegradable COD (CR), while ammonium (NH_4^+) and orthophosphate (IP) are incorporated in the biomass.
- **Anoxic bacteria growth using nitrate and nitrite.** This process produces dinitrogen (due to **denitrification**) (N_2). Both processes consume readily biodegradable COD (CR), ammonium (NH_4^+), and orthophosphate (IP). The inclusion of both processes is necessary due to the two-step nitrification model.
- **Lysis of heterotrophic organisms.** Lysis produces organic matter (readily CR, slowly CS, and inert CI COD), ammonium (NH_4^+), and orthophosphate (IP).

Autotrophic bacteria are responsible for nitrification, which is modelled as a two-step process. Both steps of the nitrification are strictly aerobic and can therefore only occur when dissolved oxygen is available.

- **Aerobic growth of Nitrosomonas.** This process consumes ammonium (NH_4^+) and oxygen (O_2), and produces nitrite (NO_2^-). Orthophosphate (IP) and a small portion of ammonium (NH_4^+) are incorporated in the biomass.
- **Aerobic growth of Nitrobacter.** This process consumes nitrite (NO_2^-) and produces nitrate (NO_3^-). Ammonium (NH_4^+) and orthophosphate IP) are incorporated in the biomass.
- Similarly to lysis of heterotrophic organisms, **lysis of autotrophic bacteria** produces organic matter (readily CR, slowly CS, and inert CI COD), ammonium (NH_4^+), and orthophosphate (IP).

Table 3.1 shows the main principles of CW2D. A '+' sign means that the process i (i = 1, ..., R) is increasing the concentration of the component, a '-' sign signals that the process is decreasing the concentration of the component. A 'o' sign shows that the concentration of the component is not affected by the process.

Table 3.1: CW2D – main principles.

	N	1	2	3	4	5	6	7	8	9	10	11	12
R	**processes \ components**	**O2**	**CR**	**CS**	**CI**	**XH**	**XANs**	**XANb**	**NH4N**	**NO2N**	**NO3N**	**N2N**	**IP**
Heterotrophic organisms													
1	hydrolysis	o	+	–	+	o	o	o	+	o	o	o	+
2	aerobic growth of heterotrophs on readily biodegradable COD	–	–	o	o	+	o	o	–	o	o	o	–
3	NO3-growth of heterotrophs on readily biodegradable COD	o	–	o	o	+	o	o	–	o	–	+	–
4	NO2-growth of heterotrophs on readily biodegradable COD	o	–	o	o	+	o	o	–	–	o	+	–
5	lysis	o	+	+	+	–	o	o	+	o	o	o	+
Nitrosomonas													
6	aerobic growth of N.somonas on NH4	–	o	o	o	o	+	o	–	+	o	o	–
7	lysis of N.somonas	o	+	+	+	o	–	o	+	o	o	o	+
Nitrobacter													
8	aerobic growth of N.bacter on NO2	–	o	o	o	o	o	+	–	–	+	o	–
9	lysis of N.bacter	o	+	+	+	o	o	–	+	o	o	o	+

+ = process R increases component N; – = process R decreases component N; o = process R has no affect on component N.

Table 3.2 is obtained by replacing the '+' and '–' symbols in Table 3.1 with stoichiometric coefficients of reactions. Table 3.2 represents the stoichiometric matrix of CW2D. A detailed description of the stoichiometric coefficients is given in Table 3.5. The concept of yield coefficients is used to describe biomass growth. The yield coefficient represents the amount of organic matter that is used for biomass growth. The stoichiometric coefficients (including the yield coefficients) that appear in Table 3.2 are defined, together with their default values, in Table 3.5 (for organic matter and micro-organisms), Table 3.6 (for ammonium nitrogen), and Table 3.7 (for inorganic phosphorus).

Table 3.2: Stoichiometric matrix of reactions in CW2D.

	N	1	2	3	4	5	6	7	8	9	10	11	12
	components	**O2**	**CR**	**CS**	**CI**	**XH**	**XANs**	**XANb**	**NH4N**	**NO2N**	**NO3N**	**N2N**	**IP**
R	**processes** \ units	gO2	gCOD	gCOD	gCOD	gCOD	gCOD	gCOD	gN	gN	gN	gN	gP
Heterotrophic organisms													
1	hydrolysis		$1-f_{Hyd,CI}$	-1	$f_{Hyd,CI}$				$\nu_{1,N}$				$\nu_{1,P}$
2	aerobic growth of heterotrophs on readily biodegradable COD	$1 - 1/Y_H$	$-1/Y_H$			1			$\nu_{2,N}$				$\nu_{2,P}$
3	NO3-growth of heterotrophs on readily biodegradable COD		$-1/Y_H$			1			$\nu_{3,N}$		$-(1-Y_H)/2.86Y_H$	$(1-Y_H)/2.86Y_H$	$\nu_{3,P}$
4	NO2-growth of heterotrophs on readily biodegradable COD		$-1/Y_H$			1			$\nu_{4,N}$	$-(1-Y_H)/1.71Y_H$		$(1-Y_H)/1.71Y_H$	$\nu_{4,P}$
5	lysis		$f_{BM,CR}$	$1-f_{BM,CR}-f_{BM,CI}$	$f_{BM,CI}$	-1			$\nu_{5,N}$				$\nu_{5,P}$
Nitrosomonas													
6	aerobic growth of N.somonas on NH4	$-(3.43-Y_{ANs})/Y_{ANs}$					1		$i_{N,BM}-1/Y_{ANs}$	$1/Y_{ANs}$			$\nu_{6,P}$
7	lysis of N.somonas		$f_{BM,CR}$	$1-f_{BM,CR}-f_{BM,CI}$	$f_{BM,CI}$		-1		$\nu_{7,N}$				$\nu_{7,P}$
Nitrobacter													
8	aerobic growth of N.bacter on NO2	$-(1.14-Y_{ANb})/Y_{ANb}$						1	$\nu_{8,N}$	$-1/Y_{ANb}$	$1/Y_{ANb}$		$\nu_{8,P}$
9	lysis of N.bacter		$f_{BM,CR}$	$1-f_{BM,CR}-f_{BM,CI}$	$f_{BM,CI}$			-1	$\nu_{9,N}$				$\nu_{9,P}$

See Table 3.5, Table 3.6, and Table 3.7 for definitions of the stoichiometric coefficients.

Equations for the process reaction rates, rc_j, are given in Table 3.3. It is assumed that reactions take place only in the aqueous phase. Therefore the overall reaction term r_i for component i can be calculated as follows:

$$r_i = \theta \cdot \sum_{j=1}^{R} \upsilon_{j,i} rc_j \tag{3.1}$$

where i = 1, ..., N (N is the number of components), j = 1, ..., R (R is the number of processes), and where r_i is the reaction term for component i [$mg_i/(dm^3_s.h)$], θ is the volumetric water content [m^3_w/m^3_s], $\upsilon_{j,i}$ is the stoichiometric factor for component i and process j [mg_i/mg_j] (Table 3.2), and rc_j is the zero-order reaction rate for process j in the aqueous phase [$mg_j/(dm^3_w.h)$] (Table 3.3). Rate coefficients and kinetic parameters that appear in Table 3.3 are defined, together with their values, in Table 3.8.

The total number of parameters of CW2D is 46 (26 kinetic parameters (Table 3.8), 6 stoichiometric parameters (Table 3.5), 8 composition parameters (Table 3.4), 2 parameters describing the oxygen transfer between gaseous and aqueous phase (Table 3.10), and 4 parameters describing the temperature dependency of the kinetic parameters (Table 3.9). Additionally, the material, diffusion, and adsorption parameters for each component, as already implemented in HYDRUS-2D, have to be specified as well.

Table 3.3: Reaction rates in CW2D.

R	Process / Reaction rate rc_j
Heterotrophic organisms	
1	Hydrolysis $rc_1 = K_h \cdot \frac{c_{CS}/c_{XH}}{K_X + c_{CS}/c_{XH}} \cdot c_{XH}$ (3.2)
2	Aerobic growth of heterotrophs on readily biodegradable COD $rc_2 = \mu_H \cdot \frac{c_{O2}}{K_{Het,O2} + c_{O2}} \cdot \frac{c_{CR}}{K_{Het,CR} + c_{CR}} \cdot f_{N,Het} \cdot c_{XH}$ (3.3)
3	NO3-growth of heterotrophs on readily biodegradable COD $rc_3 = \mu_{DN} \cdot \frac{K_{DN,O2}}{K_{DN,O2} + c_{O2}} \cdot \frac{c_{NO3}}{K_{DN,NO3} + c_{NO3}} \cdot \frac{K_{DN,NO2}}{K_{DN,NO2} + c_{NO2}} \cdot \frac{c_{CR}}{K_{DN,CR} + c_{CR}} \cdot f_{N,DN} \cdot c_{XH}$ (3.4)
4	NO2-growth of heterotrophs on readily biodegradable COD $rc_4 = \mu_{DN} \cdot \frac{K_{DN,O2}}{K_{DN,O2} + c_{O2}} \cdot \frac{c_{NO2}}{K_{DN,NO2} + c_{NO2}} \cdot \frac{c_{CR}}{K_{DN,CR} + c_{CR}} \cdot f_{N,DN} \cdot c_{XH}$ (3.5)
5	Lysis of heterotrophs $rc_5 = b_H \cdot c_{XH}$ (3.6)
Autotrophic organisms 1 – *Nitrosomonas*	
6	Aerobic growth of *Nitrosomonas* on NH4 $rc_6 = \mu_{ANs} \cdot \frac{c_{O2}}{K_{ANs,O2} + c_{O2}} \cdot \frac{c_{NH4}}{K_{ANs,NH4} + c_{NH4}} \cdot \frac{c_{IP}}{K_{ANs,IP} + c_{IP}} \cdot c_{XANs}$ (3.7)
7	Lysis of *Nitrosomonas* $rc_7 = b_{HANs} \cdot c_{XANs}$ (3.8)
Autotrophic organisms 2 – *Nitrobacter*	
8	Aerobic growth of *Nitrobacter* on NO2 $rc_8 = \mu_{ANb} \cdot \frac{c_{O2}}{K_{ANb,O2} + c_{O2}} \cdot \frac{c_{NO2}}{K_{ANb,NO2} + c_{NO2}} \cdot f_{N,ANb} \cdot c_{XANb}$ (3.9)
9	Lysis of *Nitrobacter* $rc_9 = b_{HANb} \cdot c_{XANb}$ (3.10)
Conversion of solid in liquid phase concentrations	
	$c_{XY} = \frac{\rho}{\theta} \cdot s_{XY}$, where $Y = H, ANs, ANb$ (3.11)
Factor for nutrients	
	$f_{N,x} = \frac{c_{NH4}}{K_{x,NH4} + c_{NH4}} \cdot \frac{c_{IP}}{K_{x,IP} + c_{IP}}$, where $x = Het, DN, ANb$ (3.12)

See Table 3.8 for definitions of rate coefficients.

3.3 Parameters of CW2D

In this chapter we describe parameters of CW2D that are used as default parameters. Users of the model can, however, specify their own values in the input that may be different from those given below.

3.3.1 Composition parameters

Values of composition parameters used in CW2D are taken from Henze et al. (1995) and are given in Table 3.4. The composition parameters provide information about the nitrogen and phosphorus contents of the organic matter and biomass, and therefore are measures of the mass of organic nitrogen and organic phosphorus, respectively.

Table 3.4: The composition parameters (Henze et al., 1995).

Composition parameters		Value
$i_{N,CR}$	N content of CR [$mg_N/mg_{COD,CR}$]	0.03
$i_{N,CS}$	N content of CS [$mg_N/mg_{COD,CS}$]	0.04
$i_{N,CI}$	N content of CI [$mg_N/mg_{COD,CI}$]	0.01
$i_{N,BM}$	N content of biomass [$mg_N/mg_{COD,BM}$]	0.07
$i_{P,CR}$	P content of CR [$mg_P/mg_{COD,CR}$]	0.01
$i_{P,CS}$	P content of CS [$mg_P/mg_{COD,CS}$]	0.01
$i_{P,CI}$	P content of CI [$mg_P/mg_{COD,CI}$]	0.01
$i_{P,BM}$	P content of biomass [$mg_P/mg_{COD,BM}$]	0.02

3.3.2 Stoichiometric parameters

Values of the stoichiometric parameters used in CW2D are given in Table 3.5.

Table 3.5: The stoichiometric parameters for organic matter and micro-organisms (Henze et al., 1995).

Stoichiometric parameters		Value
$f_{Hyd,CI}$	Production of CI in hydrolysis [$mg_{COD,CI}/mg_{COD,CS}$]	0
$f_{BM,CR}$	Fraction of CR generated in biomass lysis [$mg_{COD,CR}/mg_{COD,BM}$]	0.05
$f_{BM,CI}$	Fraction of CI generated in biomass lysis [$mg_{COD,CI}/mg_{COD,BM}$]	0.1
Y_H	Yield coefficient for heterotrophs [$mg_{COD,BM}/mg_{COD,CR}$]	0.63
Y_{ANs}	Yield coefficient for N.somonas [$mg_{COD,BM}/mg_{NH4N}$]	0.24*
Y_{ANb}	Yield coefficient for N.bacter [$mg_{COD,BM}/mg_{NO2N}$]	0.24*

* from Nowak (1996)

Kadlec and Knight (1996) gave for biomass growth related to organic dry matter (ODM) a value of the stoichiometric parameter of $0.17 g_{ODM}/g_{NH4N}$ for the total nitrification process. Using the ratio of the biomass dry weight (DW) to biomass COD of $0.7 g_{DW,BM}/g_{COD,BM}$ (Lazarova and Manem, 1995), one gets the same stoichiometric parameter of $0.24 g_{COD,BM}/g_{NH4N}$, as used by Nowak (1996).

Other values reported in literature include: For example, Pirsing and Wiesmann (1994) provided the yield coefficients related to organic dry matter (ODM). For Nitrosomonas and Nitrobacter the yield coefficients are $0.147 g_{ODM}/g_{NH3N}$ and $0.048 g_{ODM}/g_{NO2N}$, respectively.

Using the ratio of Lazarova and Manem (1995) one gets a yield coefficients of $0.21 g_{COD,BM}/g_{NH4N}$ for Nitrosomonas and $0.07 g_{COD,BM}/g_{NO2N}$ for Nitrobacter. Jacob et al. (1997) modelled a biofilter for wastewater treatment as a series of completely mixed tanks. They used the hydraulic model coupled to a reactive transport model based on the ASM1. They determined the yield coefficient for the heterotrophic bacteria to be $0.67 g_{COD,BM}/g_{COD,CR}$.

Stoichiometric parameters for ammonium nitrogen, $\nu_{1,N}$ to $\nu_{9,N}$, and inorganic phosphorus, $\nu_{1,P}$ to $\nu_{9,P}$, in Table 3.2 can be calculated from the mass balance equations. These mass balance equations can be written for each process j as follows:

$$\sum_{i=1}^{N} \nu_{j,i} \cdot i_{c,i} = 0 \qquad (3.13)$$

where i = 1, ..., N, with N being the number of components, j = 1, ..., R, with R being the number of processes, $\upsilon_{j,i}$ is the stoichiometric factor for component i and process j [mg_i/mg_j], c represents the material to which the mass balance is applied (either N or P), and $i_{c,i}$ is the conversion factor that converts the unit of component i to the unit of material c. The resulting equations for the stoichiometric coefficients $\nu_{j,N}$, and $\nu_{j,P}$ are given in Table 3.6 and Table 3.7, respectively.

Table 3.6: Stoichiometric coefficients for ammonium nitrogen.

$\nu_{1,N}$ =	$i_{N,CS} - (1-f_{Hyd,CI}) \cdot i_{N,CR} - f_{Hyd,CI} \cdot i_{N,CI}$
$\nu_{2,N}$ =	$1/Y_H \cdot i_{N,CR} - i_{N,BM}$
$\nu_{3,N}$ =	$1/Y_H \cdot i_{N,CR} - i_{N,BM}$
$\nu_{4,N}$ =	$1/Y_H \cdot i_{N,CR} - i_{N,BM}$
$\nu_{5,N}$ =	$i_{N,BM} - (1 - f_{BM,CR} - f_{BM,CI}) \cdot i_{N,CS} - f_{BM,CR} \cdot i_{N,CR} - f_{BM,CI} \cdot i_{N,CI}$
$\nu_{6,N}$ =	$- 1/Y_{ANs} - i_{N,BM}$
$\nu_{7,N}$ =	$i_{N,BM} - (1 - f_{BM,CR} - f_{BM,CI}) \cdot i_{N,CS} - f_{BM,CR} \cdot i_{N,CR} - f_{BM,CI} \cdot i_{N,CI}$
$\nu_{8,N}$ =	$- i_{N,BM}$
$\nu_{9,N}$ =	$i_{N,BM} - (1 - f_{BM,CR} - f_{BM,CI}) \cdot i_{N,CS} - f_{BM,CR} \cdot i_{N,CR} - f_{BM,CI} \cdot i_{N,CI}$

(3.14)

See Table 3.4 and Table 3.5 for definitions of the composition and stoichiometric parameters, respectively.

Table 3.7: Stoichiometric coefficients for inorganic phosphorus.

$\nu_{1,P}$ =	$i_{P,CS} - (1-f_{Hyd,CI}) \cdot i_{P,CR} - f_{Hyd,CI} \cdot i_{P,CI}$
$\nu_{2,P}$ =	$1/Y_H \cdot i_{P,CR} - i_{P,BM}$
$\nu_{3,P}$ =	$1/Y_H \cdot i_{P,CR} - i_{P,BM}$
$\nu_{4,P}$ =	$1/Y_H \cdot i_{P,CR} - i_{P,BM}$
$\nu_{5,P}$ =	$i_{P,BM} - (1 - f_{BM,CR} - f_{BM,CI}) \cdot i_{P,CS} - f_{BM,CR} \cdot i_{P,CR} - f_{BM,CI} \cdot i_{P,CI}$
$\nu_{6,P}$ =	$- i_{P,BM}$
$\nu_{7,P}$ =	$i_{P,BM} - (1 - f_{BM,CR} - f_{BM,CI}) \cdot i_{P,CS} - f_{BM,CR} \cdot i_{P,CR} - f_{BM,CI} \cdot i_{P,CI}$
$\nu_{8,P}$ =	$- i_{P,BM}$
$\nu_{9,P}$ =	$i_{P,BM} - (1 - f_{BM,CR} - f_{BM,CI}) \cdot i_{P,CS} - f_{BM,CR} \cdot i_{P,CR} - f_{BM,CI} \cdot i_{P,CI}$

(3.15)

See Table 3.4 and Table 3.5 for definitions of the composition and stoichiometric parameters, respectively.

3.3.3 Kinetic parameters

Values of kinetic parameters used in CW2D are given in Table 3.8 at temperatures of 10 and 20°C. For the two-step nitrification model the values of Nowak (1996) are used. The saturation/inhibition coefficients for hydrolysis and for the first step of nitrification (NH4) are according to Langergraber (2005b).

Table 3.8: Kinetic parameters in CW2D (Henze et al., 1995).

Kinetic parameter		Value	
		20°C	10°C
K_h	hydrolysis rate constant [1/d]	3	2
K_X**	sat./inh. coeff. for hydrolysis [$mg_{COD,CS}/mg_{COD,BM}$]	0.1	0.22
μ_H	maximum aerobic growth rate on CR [1/d]	6	3
b_H	rate constant for lysis [1/d]	0.4	0.2
$K_{het,O2}$	sat./inh. coeff. for O2 [mg_{O2}/l]	0.2	0.2
$K_{het,CR}$	sat./inh. coeff. for substrate [$mg_{COD,CR}$/l]	2	2
$K_{het,NH4N}$	sat./inh. coeff. for NH4 (nutrient) [mg_{NH4N}/l]	0.05	0.05
$K_{het,IP}$	sat./inh. coeff. for P [mg_{IP}/l]	0.01	0.01
μ_{DN}	maximum denitrification rate [1/d]	4.8	2.4
$K_{DN,O2}$	sat./inh. coeff. for O2 [mg_{O2}/l]	0.2	0.2
$K_{DN,NO3N}$	sat./inh. coeff. for NO3 [mg_{NO3N}/l]	0.5	0.5
$K_{DN,NO2N}$	sat./inh. coeff. for NO2 [mg_{NO2N}/l]	0.5	0.5
$K_{DN,CR}$	sat./inh. coeff. for substrate [$mg_{COD,CR}$/l]	4	4
$K_{DN,NH4N}$	sat./inh. coeff. for NH4 (nutrient) [mg_{NH4N}/l]	0.05	0.05
$K_{DN,IP}$	sat./inh. coeff. for P [mg_{IP}/l]	0.01	0.01
μ_{ANs}*	maximum aerobic growth rate on NH4N [1/d]	0.9	0.3
b_{ANs}*	rate constant for lysis [1/d]	0.15	0.05
$K_{ANs,O2}$*	sat./inh. coeff. for O2 [mg_{O2}/l]	1	1
$K_{ANs,NH4N}$**	sat./inh. coeff. for NH4 [mg_{NH4N}/l]	0.5	5.0
$K_{ANs,IP}$	sat./inh. coeff. for P [mg_{IP}/l]	0.01	0.01
μ_{ANb}*	maximum aerobic growth rate on NO2N [1/d]	1	0.35
b_{ANb}*	rate constant for lysis [1/d]	0.15	0.05
$K_{ANb,O2}$*	sat./inh. coeff. for O2 [mg_{O2}/l]	0.1	0.1
$K_{ANb,NO2N}$*	sat./inh. coeff. for NO2 [mg_{NO2N}/l]	0.1	0.1
$K_{ANb,NH4N}$	sat./inh. coeff. for NH4 (nutrient) [mg_{NH4N}/l]	0.05	0.05
$K_{ANb,IP}$	sat./inh. coeff. for P [mg_{IP}/l]	0.01	0.01

* Nowak (1996), ** Langergraber (2005b).

3.3.4 Temperature dependencies

Due to the temperature dependency of biological processes, many parameters used in CW2D have to be considered as temperature dependent. In this work temperature dependency is considered for kinetic parameters (growth and decay rates), diffusion coefficients, and the saturation concentration of dissolved oxygen. Other parameters are assumed to be independent of temperature.

In HYDRUS-2D (Šimůnek et al., 1999) the Arrhenius equation (Stumm and Morgan, 1996) is used to describe the temperature dependence of various reaction and transport parameters:

$$a_T = a_{20°C} \cdot e^{\frac{Ea \cdot \left(T^A - T_{20}{}^A\right)}{R \cdot T^A \cdot T_{20}{}^A}} \qquad (3.16)$$

where T^A is the absolute temperature [K], a_T is the value of a particular parameter at the absolute temperature T^A, $T_{20}{}^A$ is the absolute reference temperature (20°C = 293.15K), $a_{20°C}$ is the value of a particular parameter at the reference temperature $T_{20}{}^A$, R is the universal gas constant (=8.314 J/mol/K), and Ea is the activation energy [J/mol]. The Arrhenius equation was also used by Rodrigo et al. (1997) and Wood et al. (1999), who studied the temperature effects on C-N transformations in soils and on laboratory-scale constructed wetlands, respectively.

Table 3.9 gives values of the activation energies, *Ea*, for particular transport and reaction parameters used in CW2D. It is assumed that all diffusion coefficients for the aqueous phase have the same activation energy and therefore the same temperature dependency. The temperature dependency of kinetic rates in Table 3.8 is assumed to be the same for all processes caused by heterotrophic micro-organisms and for all processes caused by autotrophic micro-organisms.

Table 3.9: Values of activation energies, *Ea*, for particular transport and reaction parameters used in CW2D.

Parameter	Temperature [°C]						*Ea*
	0	5	10	12	15	20	[J/mol]
Saturation concentration of oxygen	14.5	12.7	11.2	-	10.1	9.18	-15000
Diffusion coefficients in gas phase	6.48	-	-	7.20	-	7.69[(2)]	5700
Diffusion coefficients in aqueous phase	-	-	4.68E-4	-	-	7.20E-4	29750
Rates for heterotrophic bacteria[(1)]	-	-	1	-	-	2	47825
Rates for autotrophic bacteria[(1)]	-	-	0.35	-	-	2	69050
Hydrolysis rate[(1)]	-	-	3	-	-	6	27980

Source: Luckner and Schestakow (1991); except: [(1)] = Table 3.8 and [(2)] = calculated.

3.3.5 Biofilm parameters

Data for biofilm properties are rare, and since different authors often use different measurement procedures and techniques, their results can not be easily compared. This chapter summarises biofilm data given in the literature.

Molz et al. (1986) assumed a constant average colony size in their groundwater model. They reported that the observed colony density was 10^5colonies/cm³ and the population density was 6.10^6 bacteria per g dry matter. Zhang and Bishop (1994) and Lazarova and Manem (1995) measured the density of the biofilm to be 37mg_{BM}/cm^3_{BM}, and 25-30mg_{BM}/cm^3_{BM} respectively.

Lazarova and Manem (1995) provided also some additional numbers:

- ratio of bacteria dry matter and wet matter content = 0.20$mg_{DM,BM}/mg_{WM,BM}$;
- 50% of the organic carbon content of dry matter is assumed to be biofilm;
- organic carbon content of dry weight of biomass = 0.1 – 0.5mg TOC/mg DW_{BM}; and
- ratio of biomass dry weight and biomass COD = 0.706mg DW_{BM}/mg COD_{BM}.

3.4 Parameters of HYDRUS

3.4.1 Diffusion coefficients

Table 3.10 summarises the diffusion coefficients used in CW2D and compares them with other literature values. It is assumed that all nitrogen fractions have the same diffusion coefficient. Due to the lack of data the diffusion coefficient for inorganic phosphorus is assumed to be the same as for nitrogen. To describe the relationship of between the molecular diffusion coefficients for oxygen in the gas and water phases as a function of the water content the relationship defined by Millington and Quirk (1961) using tortuosity factors for the gas and water phase is used (as in HYDRUS-2D, Šimůnek et al., 1999).

Table 3.10: Diffusion coefficients in CW2D.

Compound	Phase	Diffusion coefficients [dm^2_s/h]				
		CW2D	L&S	B&C	H&H	M&R
Oxygen	gaseous	7.69	7.69	-	-	-
	aqueous	7.20E-04	7.20E-04	7.75E-04	8.75E-04	-
Organic matter	aqueous	4.56E-04	4.56E-04	2.50E-04	2.42E-04	9.54E-05
Ammonium nitrogen	aqueous	8.01E-04	8.01E-04	6.54E-04	7.50E-04	2.44E-04
Nitrate nitrogen	aqueous	8.01E-04	-	5.79E-04	-	5.83E-04
Other nitrogen fractions	aqueous	8.01E-04	-	-	-	-
Inorganic phosphorus	aqueous	8.01E-04	-	-	-	-

L&S (Luckner and Schestakow, 1991), B&C (Bouwer and Cobb, 1987), H&H (Horn and Hempel, 1998), M&R (Martin and Reddy, 1997).

Note that in Table 3.10, and throughout this report, we often use decimetres (dm) for length units (despite this unit not being supported by HYDRUS-3D). The reason is that 1 dm^3 is equal to 1 litre, which makes relatively easy calculations and conversions of various variables that include solute concentrations, such as solute fluxes.

The exchange of oxygen from the gas phase into the aqueous phase is described using the standard model

$$\frac{dc_{O2}}{dt} = ak_{aer,O2} \cdot \left(c_{O2,sat} - c_{O2}\right) \tag{3.17}$$

where a is the air content [m_w^3/m_s^3], $k_{aer,O2}$ is the oxygen re-aeration rate [1/h] and $c_{O2,sat}$ is the temperature dependent saturation concentration of dissolved oxygen [mg_{O2}/dm_w^3]. This term has to be added to the reaction rate constant for oxygen since this is the only way to increase the concentration of dissolved oxygen (with the exception of water flow). The value for the oxygen re-aeration rate, $k_{aer,O2}$, was chosen to be equal to $10h^{-1}$. McBride and Tanner (2000) used for surface waters an oxygen re-aeration rate, $k_{aer,O2}$,of $25h^{-1}$.

3.4.2 Adsorption parameters

Adsorption is considered for ammonium nitrogen and inorganic phosphorus. It is assumed that adsorption is a kinetic process. Table 3.11 and Table 3.12 show literature values for adsorption isotherms (linear and Freundlich) of ammonium nitrogen and inorganic phosphorus, respectively, in the soil-water environment. Values vary widely due to different substrates used in various studies.

Table 3.11: Coefficient values of linear and Freundlich isotherms for adsorption of ammonium nitrogen.

Literature coefficient values for adsorption of ammonium nitrogen in the soil-water environment			
Source	Linear isotherm	Freundlich isotherm	
	$s_{NH4N} = k_{LIN} \cdot c_{NH4N}$	$s_{NH4N} = k_{1,F} \cdot c_{NH4N} \wedge k_{2,F}$	
	k_{LIN}	$k_{1,F}$	$k_{2,F}$
Kadlec and Knight (1996)	-	14.5	0.86
Martin and Reddy (1997)	1.38	-	-
Birkinshaw and Ewen (2000)	60	-	-
Antonopoulos and Wyseure (1998)	0.25	-	-
Yamaguchi et al.(1996)[1]	2.79	2.90	0.99
DeSimeone and Howes (1998)	1.20	6.20	0.60
Kaluarachchi and Parker (1988), and Padilla et al.(1992)	0.75	-	-
McBride and Tanner (2000)[2]	-	3.0	0.50

[1] only experimental data were given, from which coefficients for isotherms were calculated;
[2] kinetic adsorption behaviour with $\omega_{NH4N} = 0.8 d^{-1}$.
c_{NH4N} and s_{NH4N} – ammonium nitrogen concentrations in the aqueous and sorbed phases, respectively, [mg/dm_w^3] and [mg/kg_s]
k_{LIN} – the distribution coefficient in the linear sorption isotherm [dm_w^3/kg_s]
$k_{1,F}$ – distribution coefficient in the nonlinear Freundlich sorption isotherm [$dm_w^3/kg_s \cdot (dm_w^3/kg_s)^b$]
$k_{2,F}$ – exponent in the nonlinear Freundlich sorption isotherm [-]

Table 3.12: Coefficient values of linear and Freundlich isotherms for adsorption of phosphorus.

Literature coefficient values for adsorption of inorganic phosphorus in the soil-water environment			
Source	Linear isotherm	Freundlich isotherm	
	$s_{IP} = k_{LIN} \cdot c_{IP}$	$s_{IP} = k_{1,F} \cdot c_{IP} \wedge k_{2,F}$	
	k_{LIN}	$k_{1,F}$	$k_{2,F}$
Kadlec and Knight (1996)	19	58	0.83
Grosse et al. (1999)	185	-	-
Gray et al.(2000)[1]	-	38	0.83
Bolton and Greenway (1999)	0.28	-	-

[1] only experimental data were given, from which coefficients for isotherms were calculated.
c_{IP} and s_{IP} – inorganic phosphorus concentrations in the aqueous and sorbed phases, respectively [mg/dm_w^3] and [mg/kg_s]
k_{LIN}, $k_{1,F}$, $k_{2,F}$ – see Table 3.11.

3.4.3 Heat transport

Since biological reactions are slower when temperature is low, the consideration of heat transport is important for constructed wetlands. While the governing heat transport equation, and its initial and boundary conditions are given in Šimůnek et al. (1999), here we will discuss only the coefficients from the governing heat transport equation.

The volumetric heat capacity of the porous medium $C(\theta)$ can be calculated as

$$C(\theta) = C_s \,.\, \theta_s + C_o \,.\, \theta_o + C_w \,.\, \theta_w + C_g \,.\, \theta_g \tag{3.18}$$

where θ_x refers to the volumetric fraction [dm_x^3/dm_s^3], C refers to the volumetric heat capacity [$kg.dm_s^2/(dm_x^3.h^2.K)$], and subscripts $x = s$, o, w, g represent the solid phase, organic matter, liquid phase (water), and gas phase. Parameters used for the volumetric fractions and for the volumetric heat capacities of solid phase, organic matter, liquid phase, and gas phase are given in Table 3.13.

Table 3.13: Parameters of the volumetric heat capacity.

Substance	x	Volumetric fraction θ_x [dm_x^3/dm_s^3]	Volumetric heat capacity C_x [J/(cm_x^3.K)]	Volumetric heat capacity C_x [$kg.m_s^2.m_x^{-3}.h^{-2}.K^{-1}$]
Air	g	(θ_S - θ)	0.0013	1.68E+10
Water	w	θ	4.19	5.43E+13
Humus	o	0	2.39	3.10E+13
Sand, wet	s	(1 - θ_S)	1.26	2.16E+13

Conversion factor: 1 J = 1 N.m = 1 $kg.m^2.s^{-2}$ = 1 kg . m^2 . 3600^2 . h^{-2} = 1.296E+07 $kg.m^2.h^{-2}$

1 J/(cm^3_x.K) = 1.296E+07 $kg.m^2.h^{-2}$. 10^6 m^{-3}_x . K^{-1} = 1.296E+13 $kg.m^{-1}.h^{-2}.K^{-1}$

The thermal conductivity function $\lambda_0(\theta)$ can be described using the empirical equation derived by Chung and Horton (1987) as follows

$$\lambda_0(\theta) = b_1 + b_2 \cdot \theta + b_3 \cdot \theta^2 \tag{3.19}$$

where $\lambda_0(\theta)$ is the thermal conductivity of the porous medium [$kg.dm_s/(h^3.K)$], and b_1, b_2, and b_3 are empirical factors. The values for b_1, b_2, and b_3 as given in HYDRUS-2D (Šimůnek et al. 1999) are used (Table 3.14).

Table 3.14: Parameters of the thermal conductivity function.

Parameter	[W/(m.K)]	[$kg.m_s.h^{-3}.K^{-1}$]
b_1	0.23	1.07E+10
b_2	-2.41	-1.12E+11
b_3	4.91	2.29E+11

Conversion factor: 1 W = 1 J/s; 1 W/(m.K) = 4.666E+10 $kg.m.h^{-3}.K^{-1}$

4 The implementation of CW2D in HYDRUS

4.1 General Remarks

CW2D has been originally developed as an extension of the HYDRUS-2D software package. Modifications of the original HYDRUS-2D code (Šimůnek et al., 1999) are described first. Then the implementation of CW2D into the HYDRUS software package (Šimůnek et al., 2006a, 2006b) is described.

4.2 Modifications of the original HYDRUS-2D program code

CW2D has been implemented in the HYDRUS-2D software package (Šimůnek et al., 1999). Version 2.11 of HYDRUS-2D supports the CW2D module. Modifications of the original HYDRUS-2D program that were necessary for the implementation of CW2D are described below. These modifications include

a) an additional source code for the CW2D module,

b) changes in the structure of the main program,

c) an additional input in the input file "`Selector.in`" and the new input file "`Options.in`",

d) a new output file ("`effluent.out`"),

e) implementation of a new boundary condition, and

f) a new iterative procedure for solving solute transport equations.

4.2.1 Modifications of the main program

Figure 4.1 shows the flow chart of the original and modified main program of HYDRUS-2D. The principle course of a simulation is as follows: after the start of the executable file the input files are read and various variables are initialised. The simulation starts at the initial time with the initial time step. Water flow is calculated first for the one time step, followed by the heat transport and the solute transport. The time step is then updated and the same procedure is repeated until the end of the simulation time is reached.

The grey rectangles in Figure 4.1 show the parts of the code where the main modifications have been made. Additional biochemical parameters needed for CW2D were added to the "`Selector.in`" input file in the new block (see description in Chapter 6.1). Some additional parameters that are not supported by the graphical interface of Hydrus-2D are read from the "`Options.in`" input file (Chapter 6.2). An additional output file providing information about effluent fluxes ("`effluent.out`", Chapter 7.1) is generated. A new boundary condition that enables to simulate flooding of the surface of the constructed wetland during the feeding was implemented (Chapter 4.2.2). Since various components in CW2D depend on each other (contrary to the original HYDRUS-2D code which considered dependence between solutes only due to sequential decay), major modifications had to be made in the iterative procedure to solve the system of coupled solute transport equations (Chapter 4.2.3).

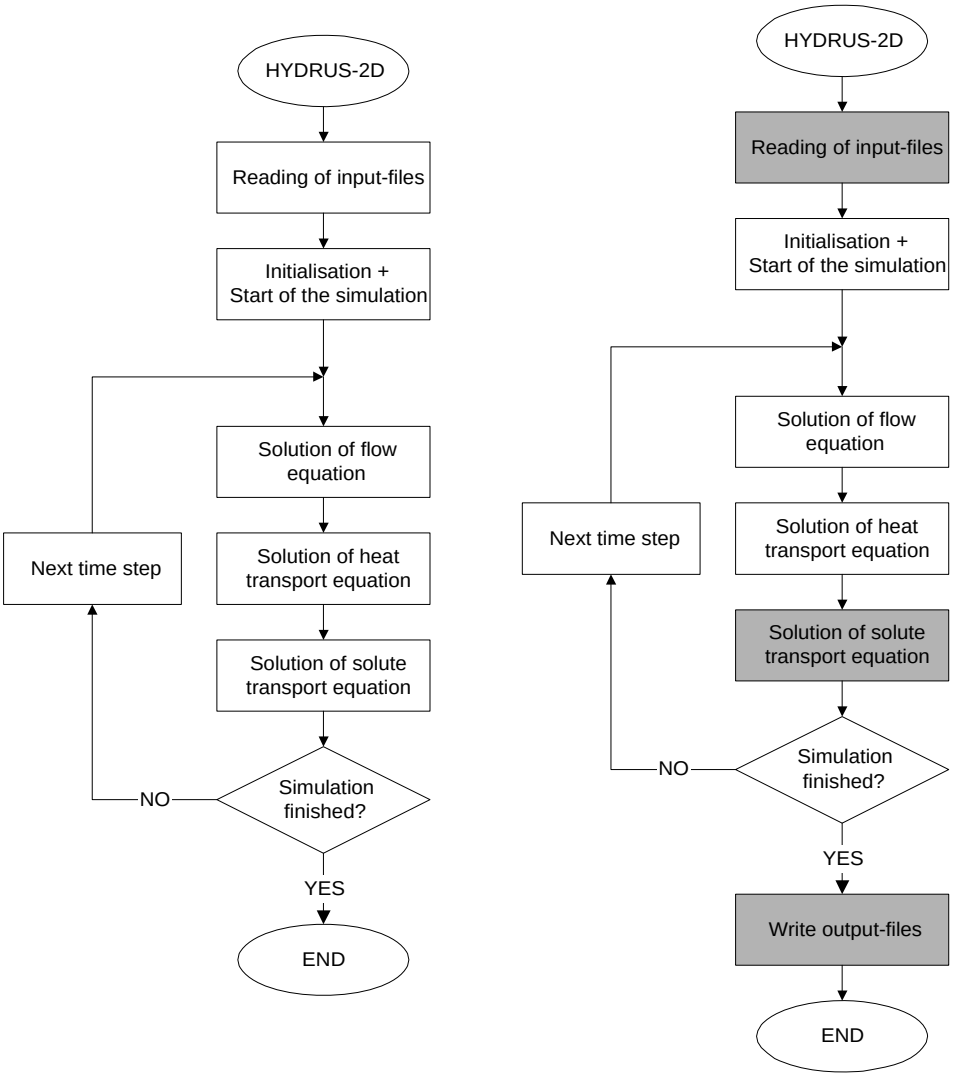

Figure 4.1: Flow chart of the original (left) and modified (right) main program of HYDRUS-2D (gray boxes represent routines that were modified to accommodate CW2D).

4.2.2 The ponding boundary condition

To describe flooding of the surface that usually occurs of during the intermittent loading of vertical flow constructed wetlands the ponding boundary condition was introduced. Ponding occurs when the infiltration capacity of the soil is smaller than the rate of loading and thus when the pressure head at the surface becomes positive and the excess water start accumulating at the soil surface. Original HYDRUS-2D assumed that no ponding occurs at the surface and that all excess water is immediately removed by the surface runs off.

The ponding boundary condition was implemented as a modification of the atmospheric boundary condition in CW2D. When 'ponding' occurs, it is assumed that water accumulates at the soil surface and that at the end of the loading period the remaining water stored on the surface infiltrates into the soil profile. The water mass balance is used to calculate the reduction of the surface pressure head until all water infiltrates into the substrate and the pressure potential at the surface becomes negative.

4.2.3 Modifications of Multi-Component Reactive Transport

The original HYDRUS-2D code considers consecutive first-order decay/degradation involving the sequential degradation of one into another solute. It was therefore possible to solve transport equations for individual species of the decay chain sequentially, since the second solute depended on the first one (and so on), but not vice versa. However, since in CW2D various components depend in a relatively complex manner on each other, all solute transport equations need to be solved simultaneously. Some major modifications thus had to be made in the iterative procedure to solve the solute transport equations simultaneously to make multi-component reactive transport possible.

The iterative procedure in the subroutine 'Solute' as implemented in the original HYDRUS-2D code is shown in the left part of Figure 4.2. During one iteration step the following subroutines are called inform the 'solute' subroutine:

- 'Disper' calculates nodal values of dispersion coefficients for solute transport,
- 'PeCour' computes the maximum local Peclet and Courant numbers and the maximum permissible time step,
- 'Coeff' calculates solute transport coefficients,
- 'SolMat' constructs the global matrix equation for solute transport,
- 'c_Bound' implements boundary conditions and determines boundary solute fluxes in boundary nodes, and finally
- the global matrix equation is solved in either ‘Orthomin” or ‘SolveT’.

Implemented chain reactions in the original version of HYDRUS-2D allowed components to be evaluated one after the other. A component could thus be influenced only by the component preceding it in the reaction chain. When convergence was reached for a particular component (needed only for nonlinear problems), the iteration procedure for a given component was finished and the calculation of the next component could be started.

This scenario changes completely when one wants to consider multi-component reactive transport where components influence each other. Necessary modifications in the 'Solute' subroutine that were needed to implement these mutual interactions between components are shown in the right part of Figure 4.2. Modified and new parts are emphasized by grey rectangles and dotted lines.

Due to the mutual interactions between components, all components have to be evaluated simultaneously at each iteration step. The iteration procedure had to be rewritten so that iteration is not done any more at the level of one single component, but must include all components simultaneously. If convergence is not reached for any component, all components have to be re-calculated during the next iteration. Additionally, evaluation of sorption processes had to be moved to the end of the iterative procedure. The sorbed concentrations can be calculated only after all liquid components are known.

The subroutine 'CW2D' (see Figure 4.2) calculates the local zero-order reaction rates rc_j (see Šimůnek et al., 1999) and the local reaction terms r_i given in Equation (3.1) using the concentrations from the previous time step. Figure 4.3 (left) shows the flow chart of the subroutine 'CW2D'. During the iteration process itself the reaction rates are assumed to be constant.

Calculated reaction terms from the ‘CW2D’ subroutine are then assigned in the 'Coeff' subroutine (Figure 4.3, right) to zero order coefficients that are then used in a usual manner to assemble the system of algebraic equations resulting from discretization of governing advection-dispersion partial differential equation.

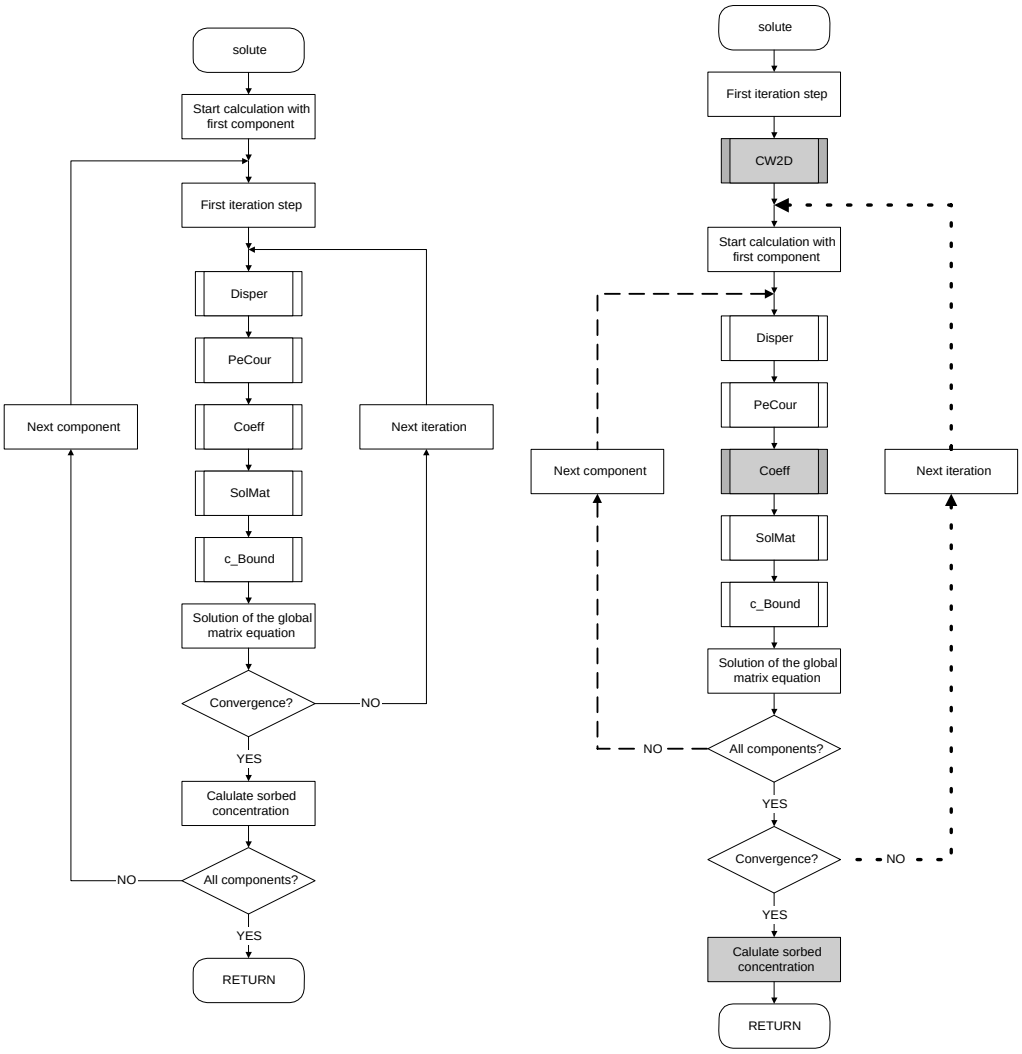

Figure 4.2: Flow chart of the original (left) and modified (right) 'Solute' subroutine.

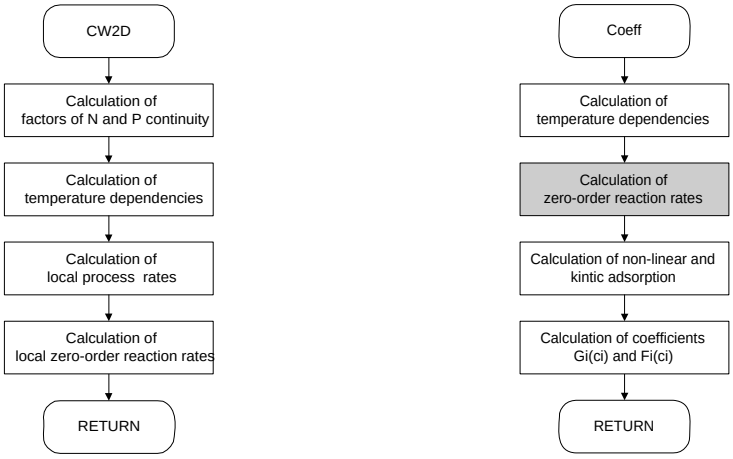

Figure 4.3: Flow chart of subroutines 'CW2D' and 'Coeff'.

4.3 The CW2D/HYDRUS user interface

4.3.1 Preliminary remarks

Concentrations units in the liquid and solid phases, as well as units of the bulk density, are fixed after choosing the length units in the "Geometry Information" window (Figure 4.4) according to Table 4.1.

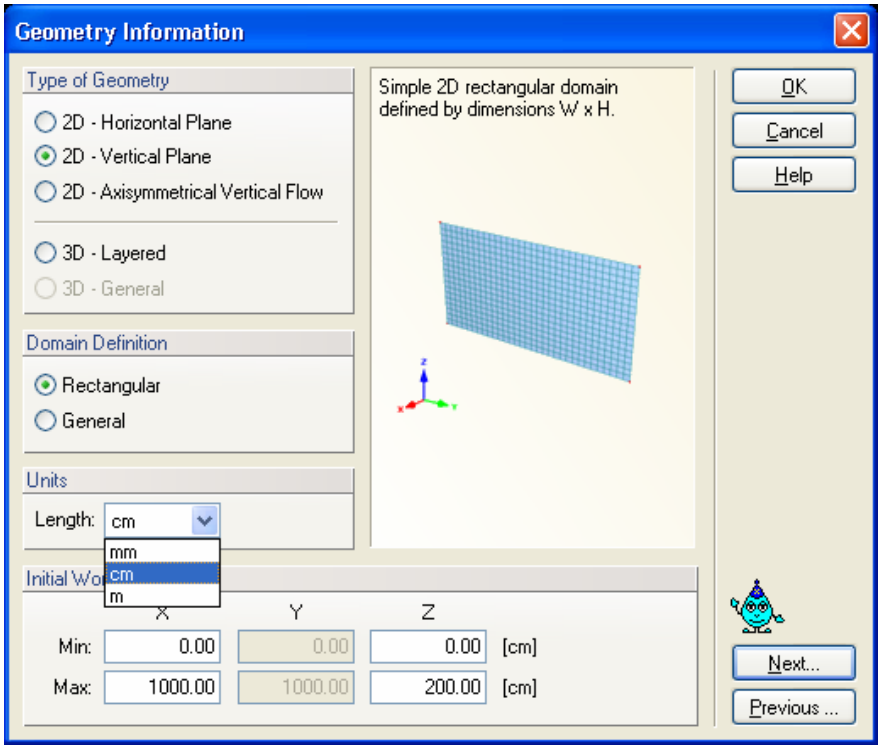

Figure 4.4: "Geometry Information" window.

Table 4.1: Units of concentrations in the liquid and solid phases and of the bulk density

Length Unit	**m**	**dm***	**cm**	**mm**
Concentrations in liquid phase	$g.m^{-3}$	$mg.dm^{-3} = mg.l^{-1}$	$\mu g.cm^{-3} = \mu g.ml^{-1}$	$ng.mm^{-3} = ng.\mu l^{-1}$
Concentrations in solid phase	$g.t^{-1}$	$mg.kg^{-1}$	$\mu g.g^{-1}$	$ng.mg^{-1}$
Bulk density	$t.m^{-3}$	$kg.dm^{-3}$	$g.cm^{-3}$	$mg.mm^{-3}$

* not supported by user interface. To use this length unit, user needs to manually rewrite the length unit at the 6th line in the '`Selector.in`' file in the temporary working directory created by HYDRUS (Šimůnek et al., 2006a).

The reactions in CW2D are implemented in the governing solute transport equations as zero-order rate constants. Based on the governing equation for macroscopic transport (e.g. Equation 3.1 in Šimůnek et al., 1999) the relationship between the units of concentrations in the liquid and solid phases is therefore defined as:

$$[c] = \left[\frac{\rho}{\theta} s \right] \tag{4.1}$$

where brackets denote units, c is the concentration in the aqueous phase [mg/dm$_w^3$], θ is the volumetric water content [dm$_w^3$/dm$_s^3$], ρ is the soil bulk density [kg$_s$/dm$_s^3$], and s is the concentration in the solid phase [mg/kg$_s$], or in units

$$\text{mg.dm}_w^{-3} = \boxed{\text{kg}_s}.\text{dm}_s^{-3} \;.\; \text{dm}_w^{-3}.\text{dm}_s^{3} \;.\; \text{mg}.\boxed{\text{kg}_s^{-1}} \qquad (4.2)$$

From Equation (4.2) it becomes clear that the unit of the bulk density has to be kg.dm^{-3}.

The HYDRUS user interface does not provide conversion of mass units, such as kg in Equation (4.2), and thus the default values of CW2D must be interpreted based on Table 4.1. Therefore units of concentrations in the liquid and solid phases and of the bulk density are fixed according to Table 4.1 once the length units are chosen.

In other figures shown in this chapter, "m" and "Days" are used as a length and time units, respectively.

4.3.2 Implementation of CW2D into the HYDRUS user interface

Pre-processing

To activate the CW2D module in the HYDRUS graphical user interface in the "Solute Transport" window (Figure 4.5) the "***Wetland Module***" box has to be ticked. The mass unit has to be set according to the chosen length unit (Table 4.1) and the number of solutes has to be set to 13 (12 CW2D module compounds and one non-reactive tracer compound, that is independent from the other 12 compounds). If the Wetland Module is chosen the "Attachment/Detachment Concept" can not be used.

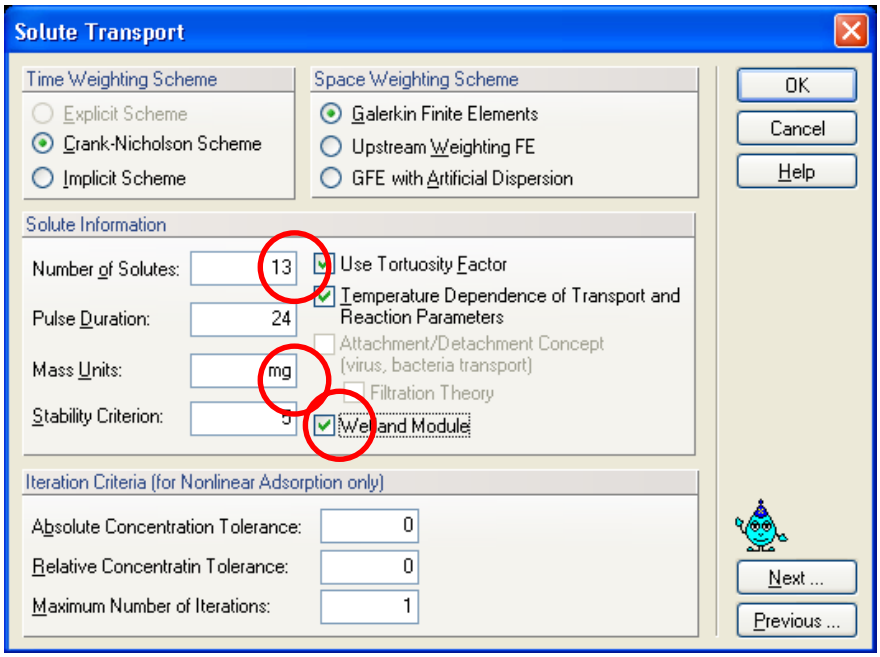

Figure 4.5: "Solute Transport" window.

Figure 4.6 shows the "Solute Transport Parameter" window where the general transport parameters are set (bulk density, dispersivity, and diffusion coefficients in the liquid and gaseous phases, chemical and physical non-equilibrium transport parameters; for description see HYDRUS manual, Simunek et al., 2006a). Figure 4.7 and Figure 4.8 show

the two user interface windows for the CW2D model parameters. For definition of particular parameters see Chapters 3.3 and 6.1, respectively.

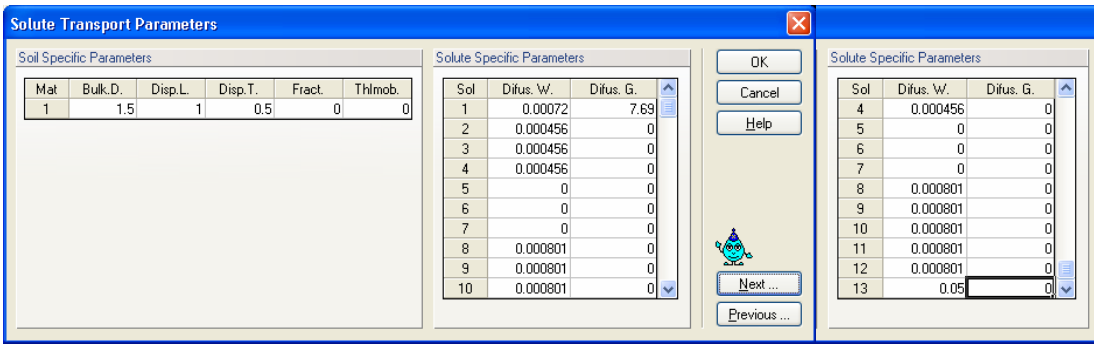

Figure 4.6: "Solute Transport Parameter" window (length unit: m; time unit: d).

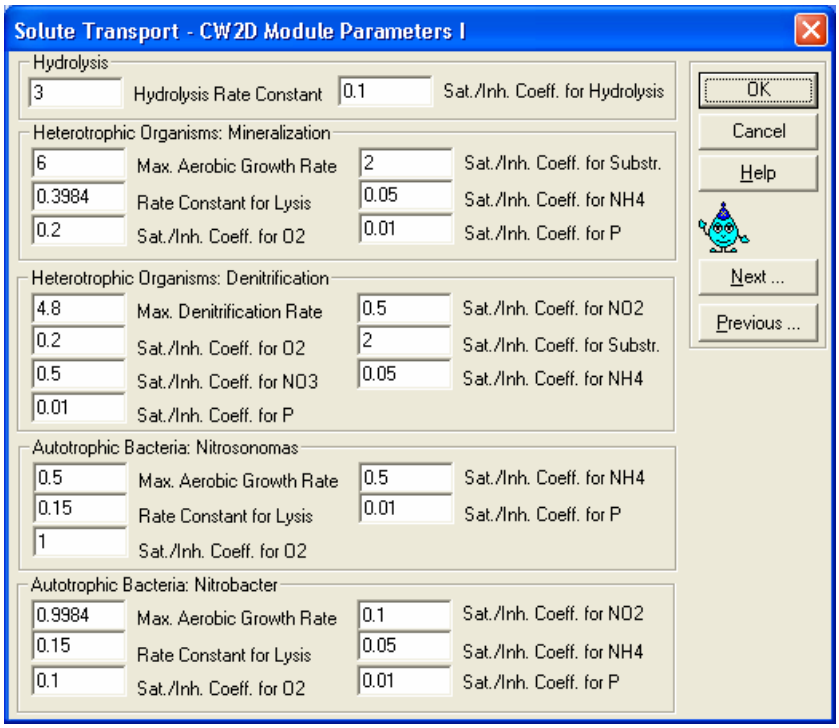

Figure 4.7: "Solute Transport – CW2D Model Parameters I" window (time unit: d).

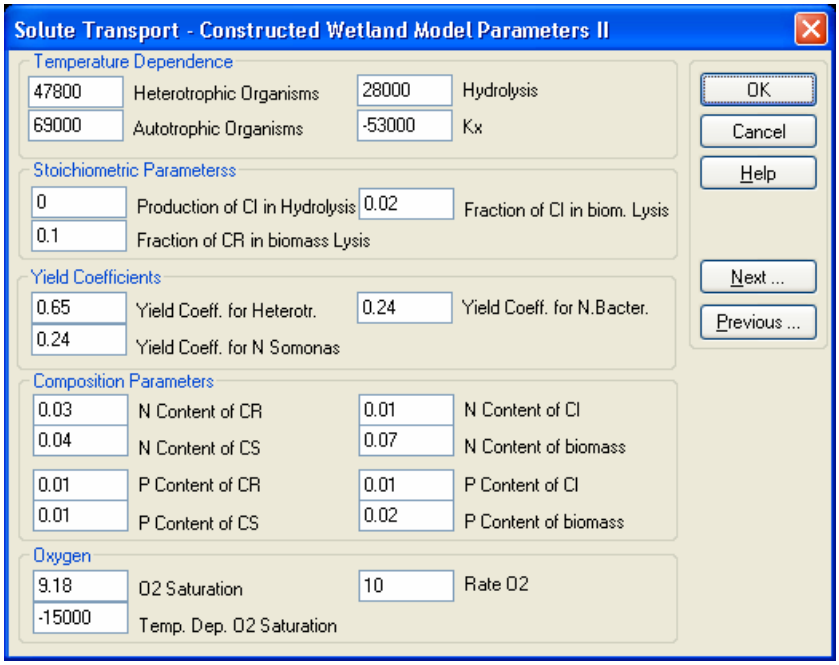

Figure 4.8: "Solute Transport – CW2D Model Parameters II" window (time unit: d).

Figure 4.9 shows the definition of the pressure head initial conditions. Names of all compounds appear under "Initial conditions" in the left sidebar, with the "L" letter denoting the concentration in the liquid phase and "S" the concentration in the solid phase.

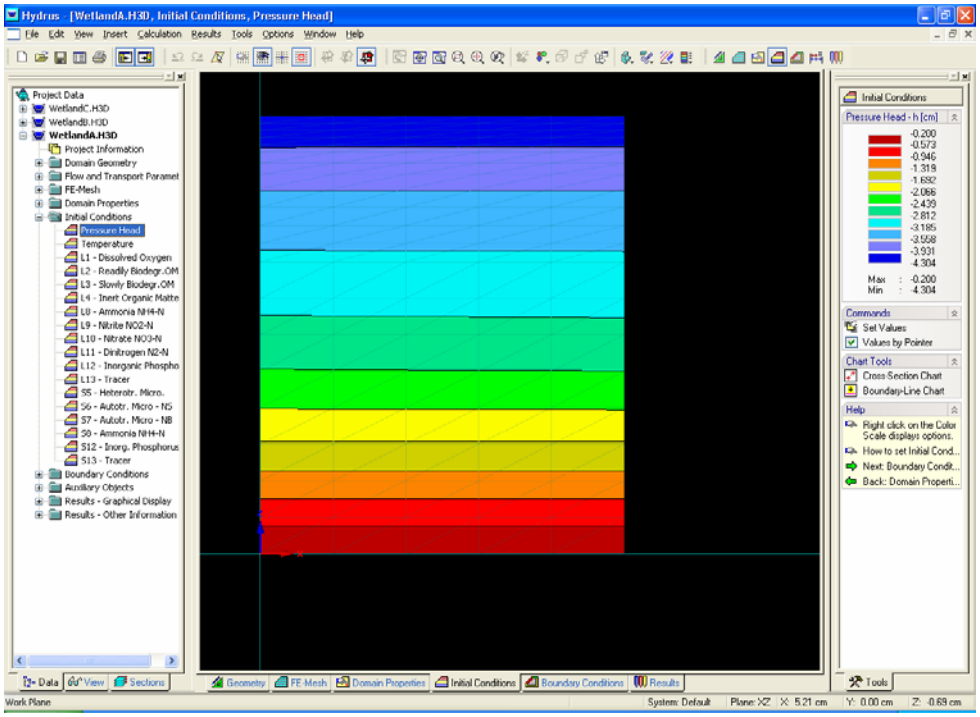

Figure 4.9: "Initial Conditions".

Post-processing

Figure 4.10 shows "Results - Graphical Display" where also the names of the compounds are shown, Figure 4.11 the "Observation Nodes" window. Again names of all variables are displayed, including all biochemical compounds.

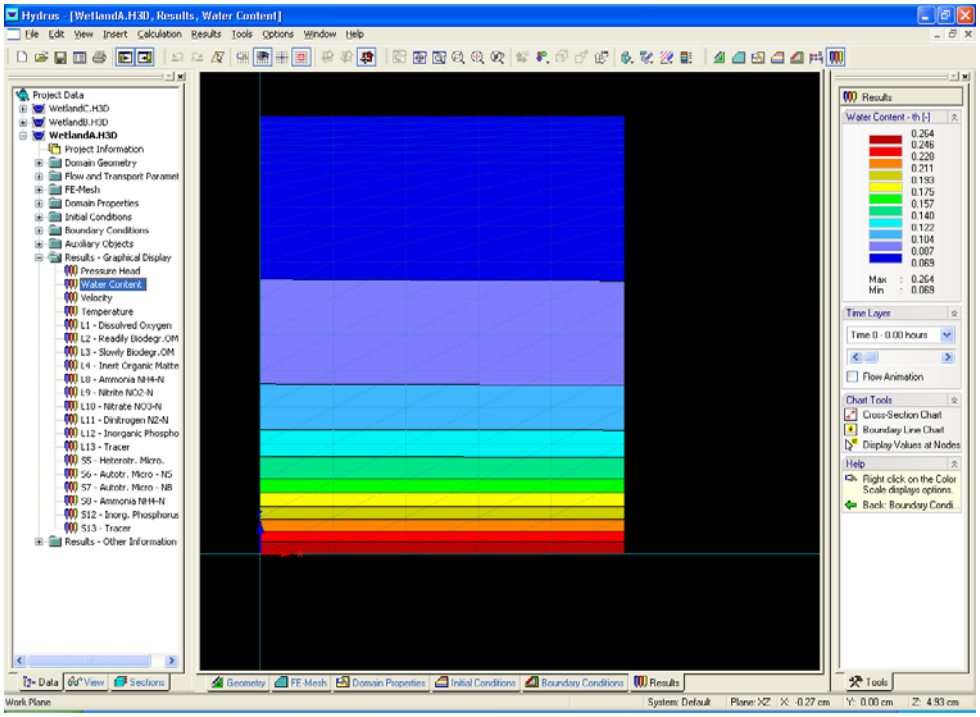

Figure 4.10: "Results - Graphical Display".

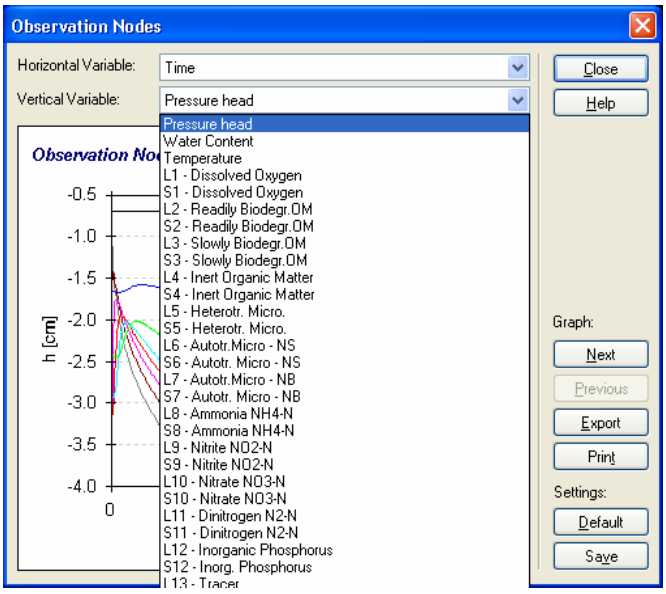

Figure 4.11: "Observation Nodes" window.

5 Examples

5.1 Pilot-scale subsurface vertical flow constructed wetland for wastewater treatment

5.1.1 System description

Figure 5.1 shows the pilot-scale subsurface constructed wetland (PSCW) that is based on Austrian standards for vertical flow constructed wetlands for wastewater treatment (ÖNORM B 2505, 1997). One PSCW has a surface area of 1 m², while five PSCW are operated in parallel (Langergraber et al., 2003). The height of the main layer of the filter bed is 60 cm. The main layer consists of sand (gravel size 0.06-4 mm or 1-4 mm, respectively). An intermediate layer of 10 cm thickness with a gravel size of 4-8 mm prevents fine particles to be washed out into the drainage layer (15 cm thick; gravel 16-32 cm) where the effluent is collected by means of tile drains.

The PSCW is loaded intermittently with wastewater. Following Austrian standards, the daily loading rate is 40 litres at application intervals of 6 hours long (i.e., a single loading comprised 10 litres). Pressure heads and water contents are measured automatically at regular time intervals at different depths (every 10 cm in the main layer). Additionally, the effluent flow rate is measured manually.

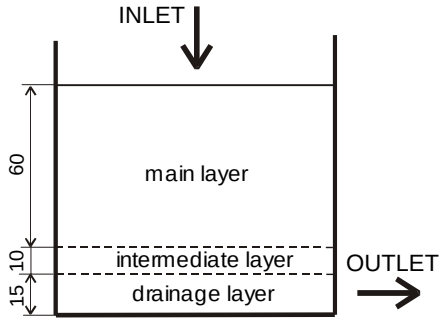

Figure 5.1: Schematic of the pilot-scale subsurface constructed wetland (values are in cm).

5.1.2 Measured data

The sandy material used for the main layer had a porosity of 0.30 and the saturated hydraulic conductivity, K_s, of 11.7 dm/h. Table 5.1 shows the measured cumulated effluent for one loading interval of 6 hours (360 minutes) and a single hydraulic loading of 10 litres.

Table 5.1. Measured cumulated effluent

Time	[min]	10	20	30	40	50	60	70	80	90	103	110
Cum. effluent	[litre]	0.16	0.31	0.48	0.64	0.80	0.99	1.20	1.49	1.87	2.39	2.67
Time	[min]	120	130	140	150	160	170	180	190	200	212	225
Cum. effluent	[litre]	3.11	3.54	3.95	4.37	4.75	5.12	5.47	5.80	6.14	6.53	6.90
Time	[min]	240	255	270	285	300	317	330	345	360	-	-
Cum. effluent	[litre]	7.31	7.70	8.08	8.45	8.78	9.16	9.43	9.70	9.99	-	-

Tracer experiments using NaCl were run for daily hydraulic loading rates of 40 and 60 litres. The electrical conductivity of the effluent, which is directly related to the tracer concentration, was measured automatically. The measured influent conductivity of the tracer was 30 $mS.cm^{-1}$, while the background conductivity during the tracer experiment was 1.5 $mS.cm^{-1}$. Influent and effluent concentrations of various nitrogen species and total organic carbon (TOC) were measured periodically. Table 5.2 shows the median values and confidence intervals of the measured influent and effluent concentrations for NH4-N, NO3-N, and TOC.

Table 5.2. Median values and confidence intervals (in parenthesis) of the measured influent and effluent concentrations of NH_4^+, NO_3^- and total organic carbon in $mg.l^{-1}$ (Langergraber, 2003).

Component	**NH_4-N**	**NO_3-N**	**TOC**
Influent	60.0 (11.2)	3.0 (0.8)	82.9 (3.5)
Effluent 0.06-4 mm substrate	0.15 (0.03)	38.5 (6.8)	3.9 (0.2)
Effluent 1-4 mm substrate	1.20 (0.31)	50.0 (8.7)	6.4 (0.3)

5.1.3 Simulation set up

The width of the transport domain was 1 m (only one half of the PSCW width is considered), and its depth is 0.6 m (only the main layer is simulated), while the transport domain itself was discretized into 6 columns and 21 rows. This results in a structured two-dimensional finite element mesh consisting of 126 nodes and 200 triangular finite elements (Figure 5.2). An atmospheric BC is assigned to the top and a constant pressure head BC (constant head of -2 cm) to the bottom of the system.

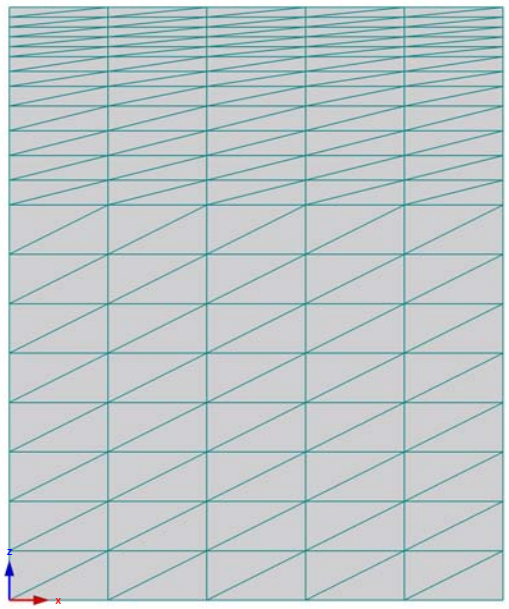

Figure 5.2: Two-dimensional finite element mesh of the PSCW.

5.1.4 Simulation results

Simulation of water flow

Table 5.3 shows various parameter sets of the van Genuchten-Mualem soil hydraulic property model used in flow simulations (Figure 5.3 and Figure 5.4). The "Literature" parameter set 1 is based on default parameters provided by HYDRUS for sand using pedotransfer functions published by Carsel and Parrish (1988). The shape factors for sand were also used for parameter set 2 in Table 5.3, but now with the measured values of the saturated water content θ_s and the saturated hydraulic conductivity K_s. Parameter set 3 in Table 5.3 was obtained by calibrating the model against cumulative effluent data, while parameter set 4 represents parameters optimized using the effluent rates. Parameter set 5 are those reported by Langergraber (2003) who, in addition to the effluent rates, also used water content measurements at 25 cm depth, while simultaneously optimizing the saturated hydraulic conductivity K_s.

Table 5.3. Literature and fitted soil hydraulic parameters of the van Genuchten-Mualem model for the 0.06-4 mm substrate.

Set	Parameter	Residual water content θ_r	Saturated water content θ_s	Parameter α	Parameter n	Parameter l	Saturated hydraulic conductivity K_s
	Unit	($dm_w^3.dm_s^{-3}$)	($dm_w^3.dm_s^{-3}$)	(dm_s^{-1})	(-)	(-)	($dm_s.h^{-1}$)
1	Literature	0.045	0.43	1.45	2.68	0.5	2.97
2	Measured K_s +θ_s	0.045	0.30	1.45	2.68	0.5	11.7
3	Fitted (1)	0.0866	0.30	1.520	2.472	0.696	11.7
4	Fitted (2)	0.0724	0.30	1.596	2.214	0.682	11.7
5	Langergraber (2003)	0.056	0.289	1.26	1.92	0.5	8.4

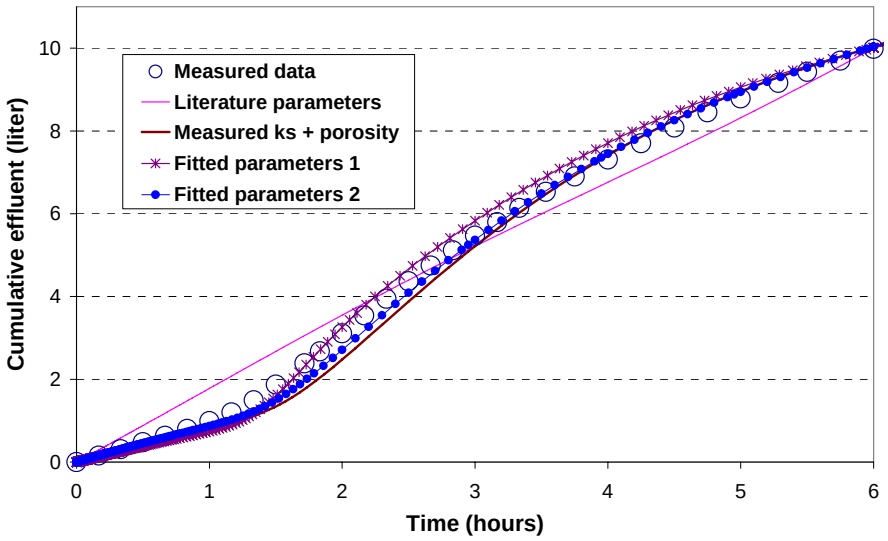

Figure 5.3: Measured and simulated cumulated effluent for a single application of 10 litres (4 loadings per day; daily hydraulic load of 40 litres).

Figure 5.3 and Figure 5.4 show the measured and simulated cumulated effluents and effluent flow rates, respectively. Simulation results are presented for parameter sets given in Table 5.3. The simulation using the fitted parameter set 3 shows a good match with the measured cumulated effluent (Figure 5.3). However, peak effluent rates are significantly

overpredicted (Figure 5.4). The Parameter set 4 describes the effluent rates much better. However, the best fit was obtained (Figure 5.5) with the parameter set of Langergraber (2003), which indicates that additional water content data and more degrees of freedom in optimization (i.e., one additional parameter was fitted) can result in a better calibration of the flow model.

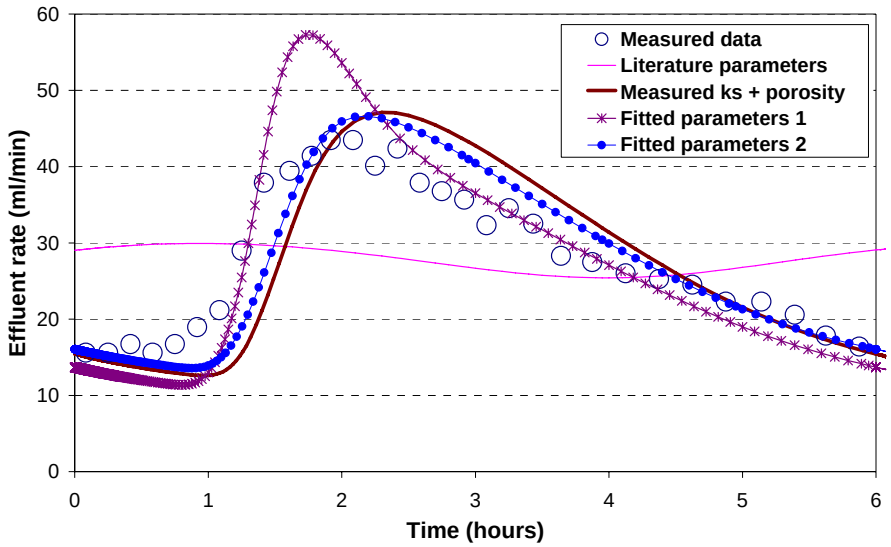

Figure 5.4: Measured and simulated effluent rates for a single application of 10 litres (4 loadings per day; daily hydraulic load of 40 litres).

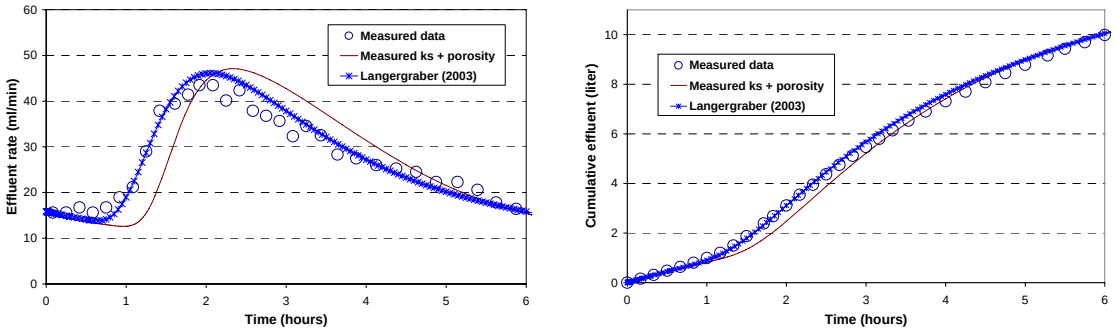

Figure 5.5: Measured and simulated effluent rates (left) and cumulated effluent (right) for a single feeding of 10 litres (4 loading per day, daily hydraulic load of 40 litres).

Figure 5.6 shows the measured and simulated effluent rates and cumulative effluents for an increased daily hydraulic loading rate of 60 litres using fitted parameter set as given by Langergraber (2003, see Table 5.3). Again, it was possible to simulate the measured hydraulic behaviour.

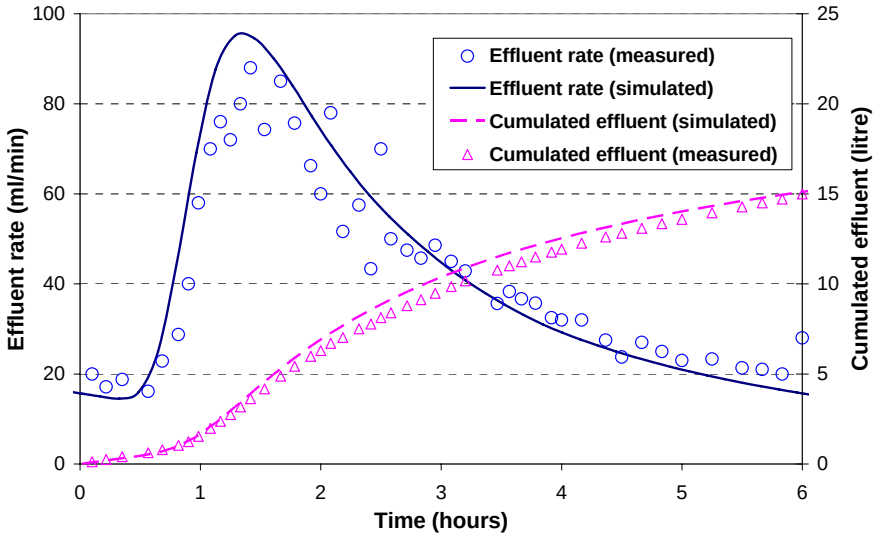

Figure 5.6: Measured and simulated effluent rates and cumulated effluent for a single feeding of 15 litres (4 loading per day, daily hydraulic load of 60 litres).

Simulation of surface ponding

Figure 5.7 shows the pressure head at the top of the constructed wetland system during a loading when ponding occurred (loading for 1 minute with 0.333 dm/minute). Positive pressure heads indicate existence of the water layer on the top of the system.

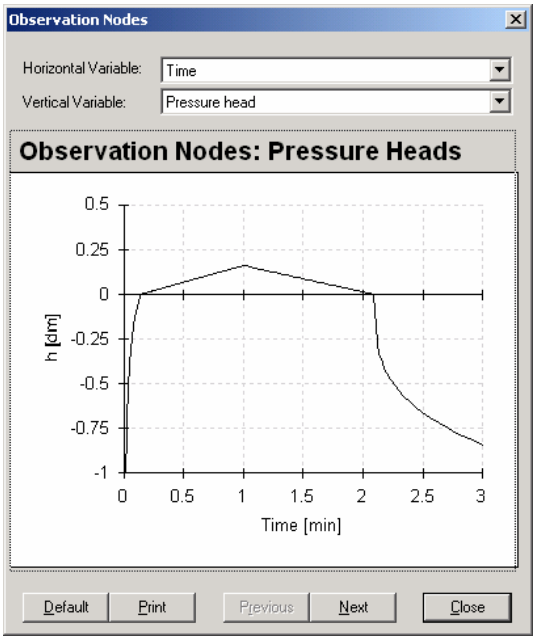

Figure 5.7: Simulated pressure heads at the top of the constructed wetland system.

Simulation of single-component solute transport

Table 5.4 shows parameters that were used for the equilibrium general solute transport model, and Table 5.5 parameters for the physical non-equilibrium transport model. The physical equilibrium transport model assumes that all pore water is mobile, whereas the physical non-equilibrium transport model considers a fraction of the pore water to be immobile (stagnant). Figure 5.8 compares simulated and measured breakthrough curves (Langergraber, 2003). For both hydraulic loading rates the simulation results matched the measured data relatively well.

Table 5.4. Parameters of the general equilibrium solute transport model

Parameter	Diffusion coefficient	Longitudinal dispersivity	Transverse dispersivity
Unit	($dm_s^2.h^{-1}$)	(dm_s)	(dm_s)
Value	0.05	0.125	0.10

Table 5.5. Parameters for the physical non-equilibrium transport model

Parameter	Fraction of sorption sites in contact with mobile water	Immobile water content	Coefficient for solute exchange between mobile and immobile water
Unit	(-)	($dm_w^3.dm_s^{-3}$)	(h^{-1})
Value	0.95	0.05	2

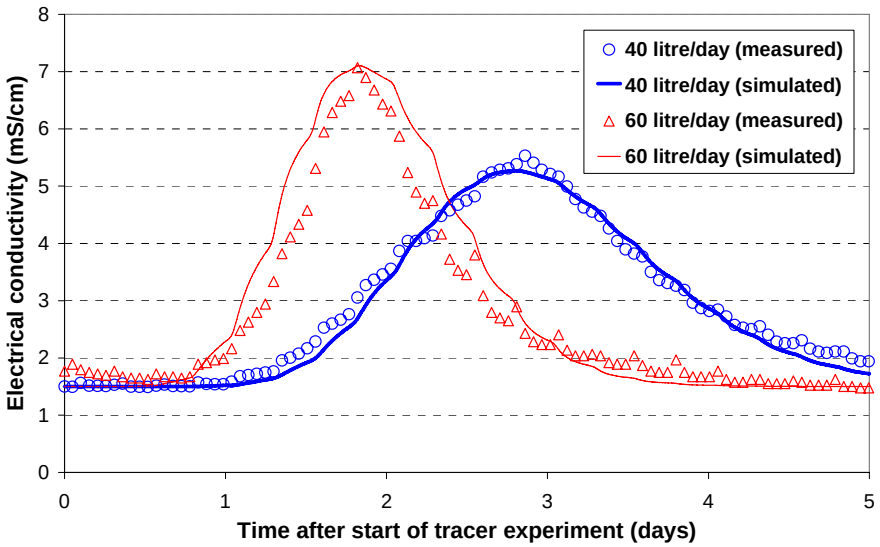

Figure 5.8: Measured and simulated effluent electrical conductivities for different daily hydraulic loads.

Simulation of multi-component reactive transport

Table 5.6 shows measured influent and effluent concentrations of selected components, as well as the influent concentrations used in the CW2D simulation, and the resulting simulated effluent concentrations. The simulated and measured effluent concentrations of ammonium nitrogen are lower for the 0.06-4 mm gravel than for the coarser material

(gravel size of 1-4 mm). The higher flow rates in the main layer with the coarse material reduce the contact time between water and the bacteria. The effluent concentrations of ammonium nitrogen, NH4N, and the slowly degradable organic matter, CS, are significantly higher for the coarser material. Effluent nitrate concentrations are also higher because of less readily degradable organic matter CR produced by hydrolysis that could be utilised for denitrification in deeper layers.

Table 5.6. Measured and simulated influent and effluent concentrations.

Component Unit	NH_4-N ($mg.l^{-1}$)	NO_3-N ($mg.l^{-1}$)	TOC ($mg.l^{-1}$)	COD ($mg_{COD}.l^{-1}$)	CR ($mg_{COD}.l^{-1}$)	CS ($mg_{COD}.l^{-1}$)
Influent						
Measured (median)	60.0	3.0	82.9	-	-	-
Simulation (input)	60.0	3.0	-	300	150	130
Effluent						
0.06-4 mm substrate						
Measured (median)	0.15	38.5	3.9	-	-	-
Simulation (median)	0.01	41.1	-	23.8	0.6	0.4
1-4 mm substrate						
Measured (median)	1.20	50.0	6.4	-	-	-
Simulation (median)	0.16	63.0	-	30.1	0.3	5.7

Results of the reactive transport simulations showed an overall good match with the measured data. This could be partly explained by the good calibration of the flow model, which was made possible by having data that provided a good definition of flow processes in the system.

Below we present several figures showing time series of the simulation results for two loadings using the "Graphical Display of Results" and the "Observation Nodes" post-processing windows, respectively. Three observation nodes are defined in 5, 15, and 50 cm depths of the system (in the 60-cm main layer). Figure 5.9 shows time series for the pressure head and dissolved oxygen. Oxygen depletion at depths of 5 and 15 cm can be observed to occur immediately after loading due to degradation. However, the oxygen concentration at 50 cm stays rather constant at a level close to the saturation concentration during the entire loading interval. After less than 2 hours the oxygen concentration at depths of 5 and 15 cm reaches saturation again.

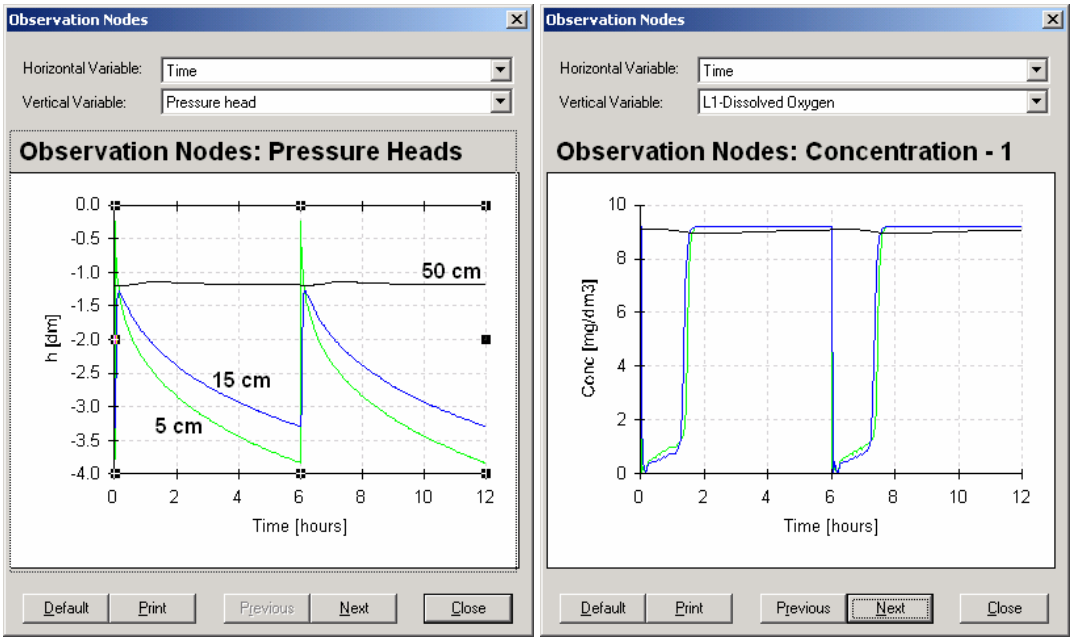

Figure 5.9: Pressure head (left) and dissolved oxygen (right).

Time series and vertical concentration profiles at the end of the simulation (12 hours) are shown in Figure 5.10 and Figure 5.11 for heterotrophic and autotrophic organisms, respectively. During two loading intervals the concentrations of the micro-organisms remained constant, thus indicating quasi steady-state conditions when growth and lysis processes are in balance (Figure 5.10 and Figure 5.11, left). Almost all micro-organisms were present in the top 20 cm of the filter (Figure 5.10 and Figure 5.11, right), where most transformations and degradation processes took place.

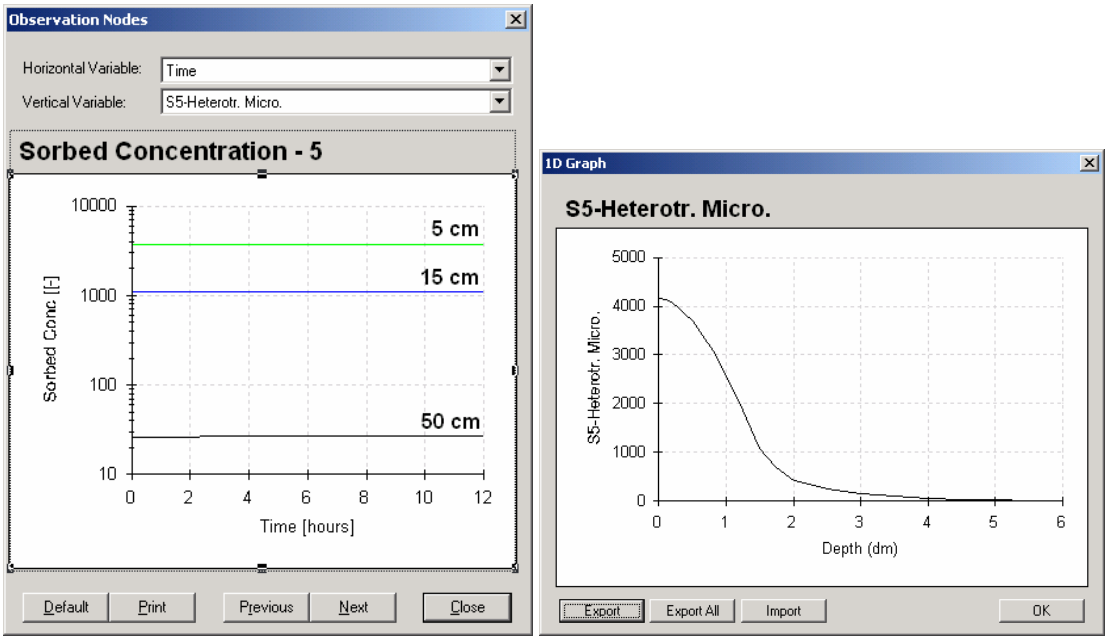

Figure 5.10: Time series (left) and vertical profile (right) of heterotrophic micro-organims.

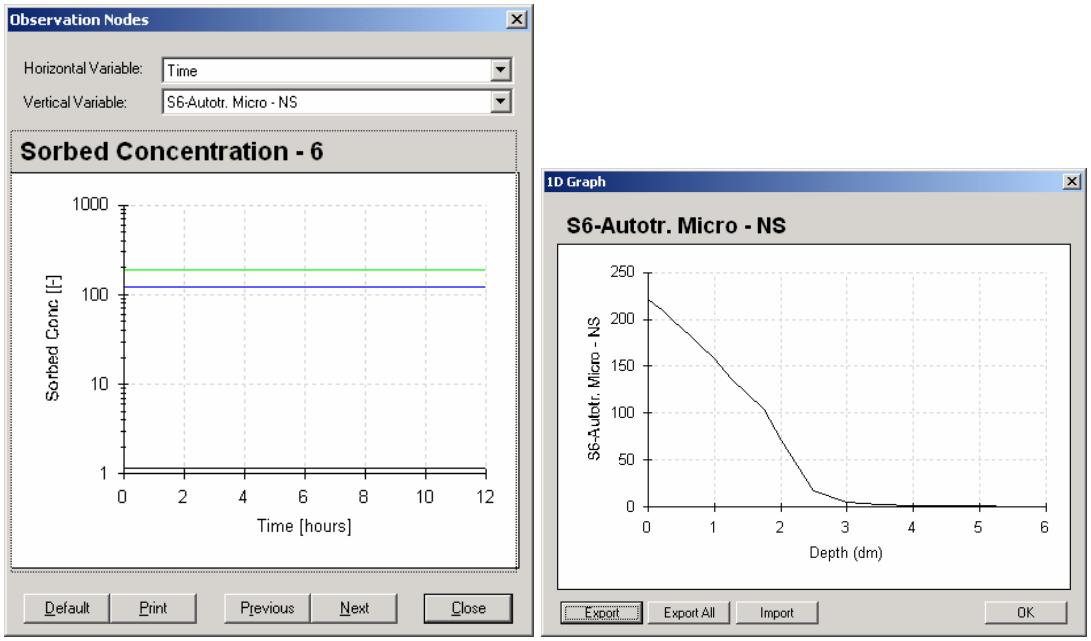

Figure 5.11: Simulated time series (left) and vertical profile (right) of autotrophic micro-organisms.

Figure 5.12 shows time series for ammonium and nitrate nitrogen, respectively. The effluent concentration for NH4N and NO3N were about 0.01 mg/l and 41 mg/l, respectively. Vertical concentration profiles at simulation times of 1 minute (end of loading), 6 minutes, 30 minutes, and 2 hours are shown in Figure 5.13 for ammonium nitrogen and in Figure 5.14 for nitrate nitrogen, respectively. Notice that the concentration peaks for NH4N at 5 and 15 cm coincide with minima in the NO3 simulations. By contrast, concentrations of NH4 and NO3 remained very stable at 50 cm depth.

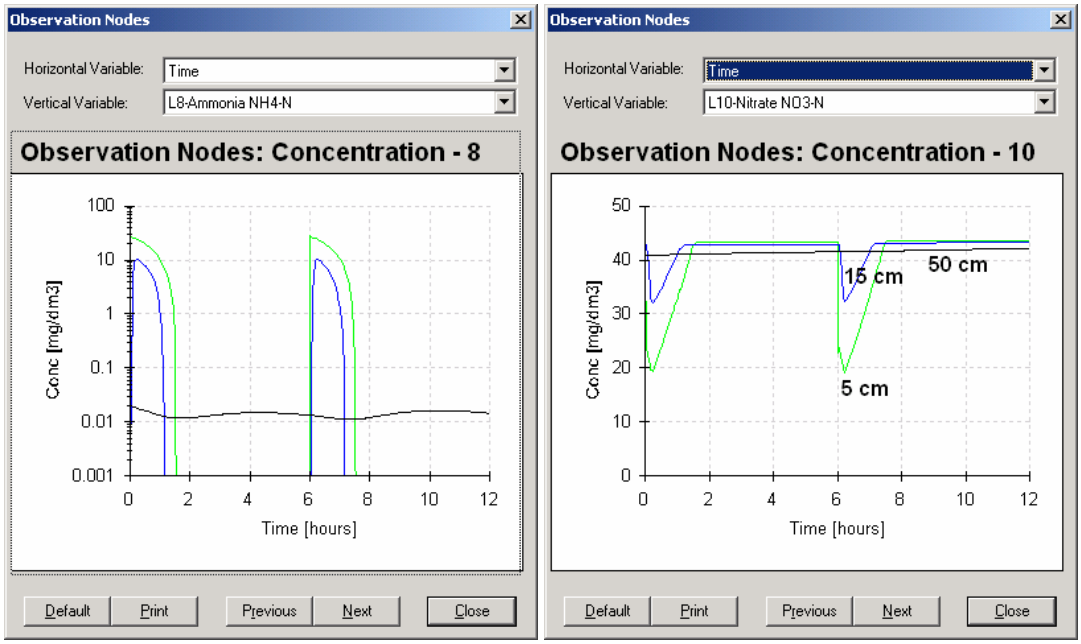

Figure 5.12: Ammonium (left) and nitrate nitrogen (right).

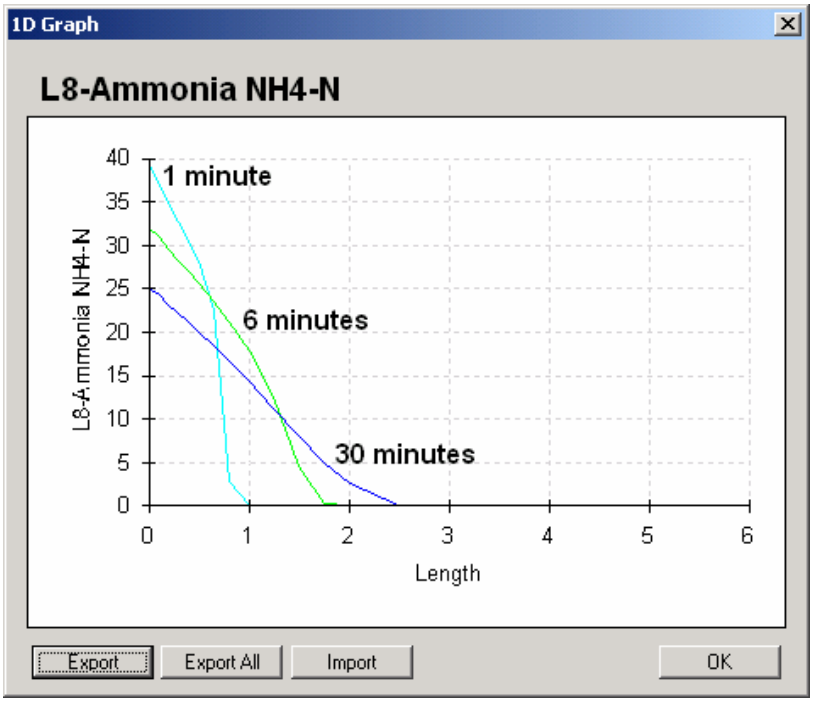

Figure 5.13: Vertical profiles of ammonium nitrogen at t = 1 minute (end of loading), 6 minutes, 30 minutes, and 2 hours.

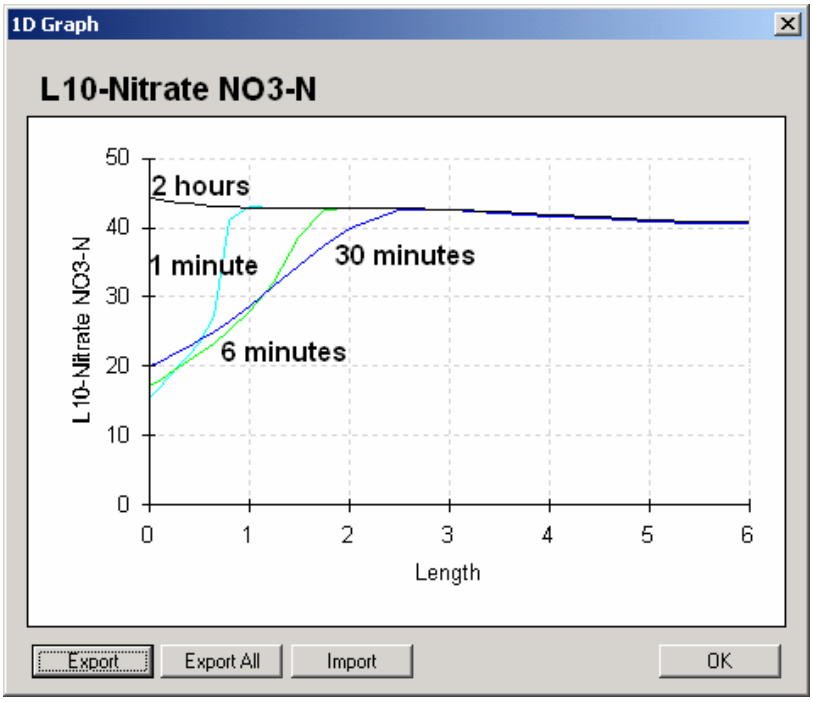

Figure 5.14: Vertical profiles of nitrate nitrogen at t = 1 minute (end of loading), 6 minutes, 30 minutes, and 2 hours.

5.2 Two-stage subsurface flow constructed wetland

5.2.1 System description

The Small-Scale Plot (SSP) system described by Grosse et al. (1999) is a pilot-scale two-stage vertical flow constructed wetland for the treatment of heavily polluted surface water. The total surface area of the SSP is 2 m², being divided into downflow and upflow chambers (each having a surface area of 1 m²). The inlet is situated on top of the downflow chamber. The effluent is collected in the upflow chamber by means of perforated pipes. A separating wall is built between the downflow and upflow chambers.

Figure 5.15 shows a schematic of the SSP (Perfler et al., 1999). Heights of the downflow and upflow chambers are 85 and 60 cm, respectively. The drainage layer at the bottom of both chambers has a height of 15 cm. This layer was connected to the two chambers and contained two tile drains. The main layers of depths of 55 and 45 cm in the downflow and upflow chambers, respectively, is filled with sand (gravel size 0.06-4 mm, 0-4 mm in Figure 5.15). The top layer of the downflow chamber has a height of 15 cm (gravel size 4-8 mm). Algae growth in the top layer was prevented by keeping the water table during application beneath the soil surface. Figure 5.16 shows sampling points in the main layer for measurements along the flow path.

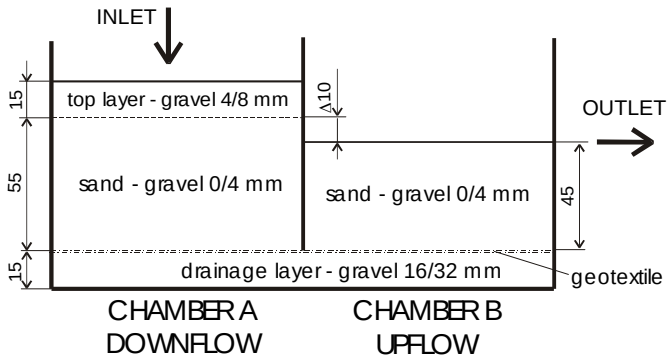

Figure 5.15: Schematic of a pilot-scale vertical flow constructed wetland (SSP) (distances are in cm).

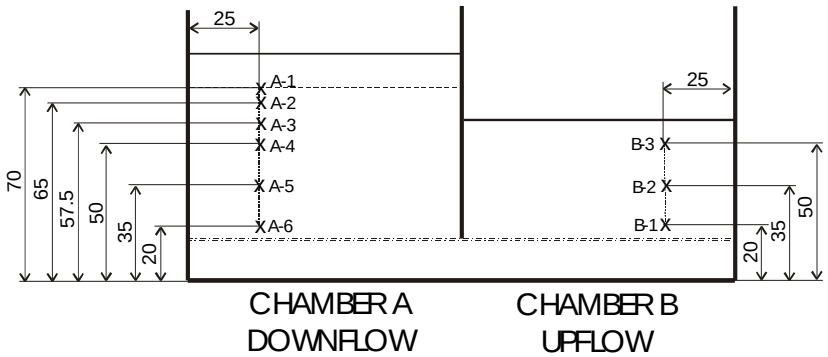

Figure 5.16: Sampling points in the main layer of the SSP (distances are in cm).

5.2.2 Simulation set up

The unstructured two-dimensional finite element mesh used for the SSP simulations consists of 1135 nodes and 2057 elements (Figure 5.17). The inlet distribution pipe at the top of the downflow chamber is modelled as a time dependent atmospheric boundary condition. Outlet (effluent) drainage pipes are modelled as circular openings in the transport domain, and subjected to seepage face boundary condition.

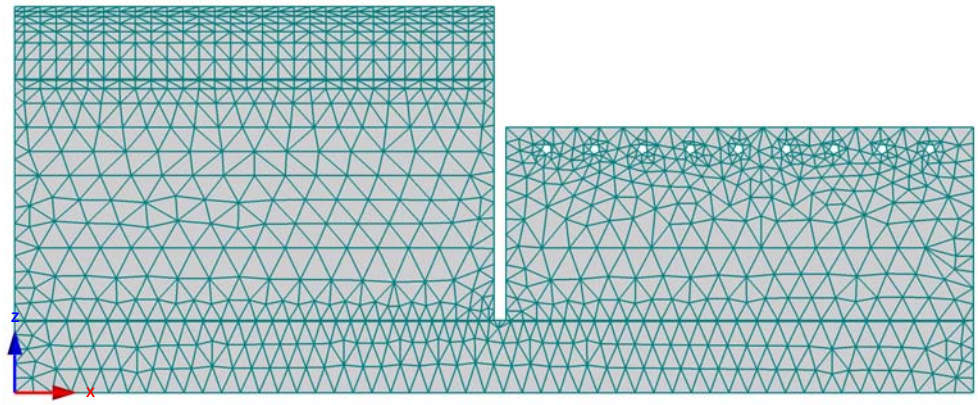

Figure 5.17: The unstructured two-dimensional finite element mesh of the SSP.

5.2.3 Simulation results

Simulation of single-component reactive transport

To show the influence of using the physical non-equilibrium transport model in comparison with the physical equilibrium transport model, simulation results are shown only for the single-component, i.e., the simulation of a tracer experiment (Langergraber, 2003).

During the tracer experiment the background electrical conductivity was 0.75 $mS.cm^{-1}$. The loading rate was 50 litres every 2 hours (i.e., 600 $litres.day^{-1}$). During the first feeding interval the conductivity of the inflow was 30 $mS.cm^{-1}$. During the following feedings the inflow conductivity was 0.75 $mS.cm^{-1}$.

Table 5.7 shows the soil hydraulic parameters of the van Genuchten-Mualem model used, Table 5.8 shows the parameters for the physical non-equilibrium transport model. The same values as shown in Table 5.4 were used for the general solute transport model parameters.

Figure 5.18 shows breakthrough curves of the simulated and measured electrical conductivities at three different sampling points and at the outlet of the SSP. The figure compares simulation results with physical equilibrium and non-equilibrium (using concept of mobile-immobile water) transport models.

Taking into account stagnant (immobile) regions of the pore water results into a better match of data by the simulation, compared to when only mobile pore water is considered. Neglecting the immobile regions leads to higher electrical conductivity values than measured (e.g. upper right graph of Figure 5.18) and to an early rise of the breakthrough

curves in the upflow chamber (Figure 5.18, lower left graph) and at the outlet (Figure 5.18, lower right graph). The observed behaviour that the effluent concentration raises earlier than the concentration in the upper sampling point of the upflow chamber (B-3) could be simulated for both, physical equilibrium and non-equilibrium transport. However, considering physical non-equilibrium transport the peak values are lower and in the range of the observed values.

Table 5.7. van Genuchten-Mualem soil hydraulic parameters for the two-stage constructed wetlands system

Parameter	Residual water content θ_r	Saturated water content θ_s	Parameter α	n	l	Saturated hydraulic conductivity K_s
Unit	($dm_w^3.dm_s^{-3}$)	($dm_w^3.dm_s^{-3}$)	(dm_s^{-1})	(-)	(-)	($dm_s.h^{-1}$)
Top layer	0.045	0.41	1.45	5.0	0.5	6000
Main layer	0.045	0.30	1.45	2.68	0.5	11.7
Drainage layer *	0.056	0.15	1.45	1.92	0.5	6000

* Drainage layer is always saturated

Table 5.8. Parameters for the physical non-equilibrium transport model

Parameter	Fraction of sorption sites in contact with mobile water	Immobile water content	Coefficient for solute exchange between mobile and immobile water
Unit	(-)	($dm_w^3.dm_s^{-3}$)	(h^{-1})
Value	0.95	0.05	2

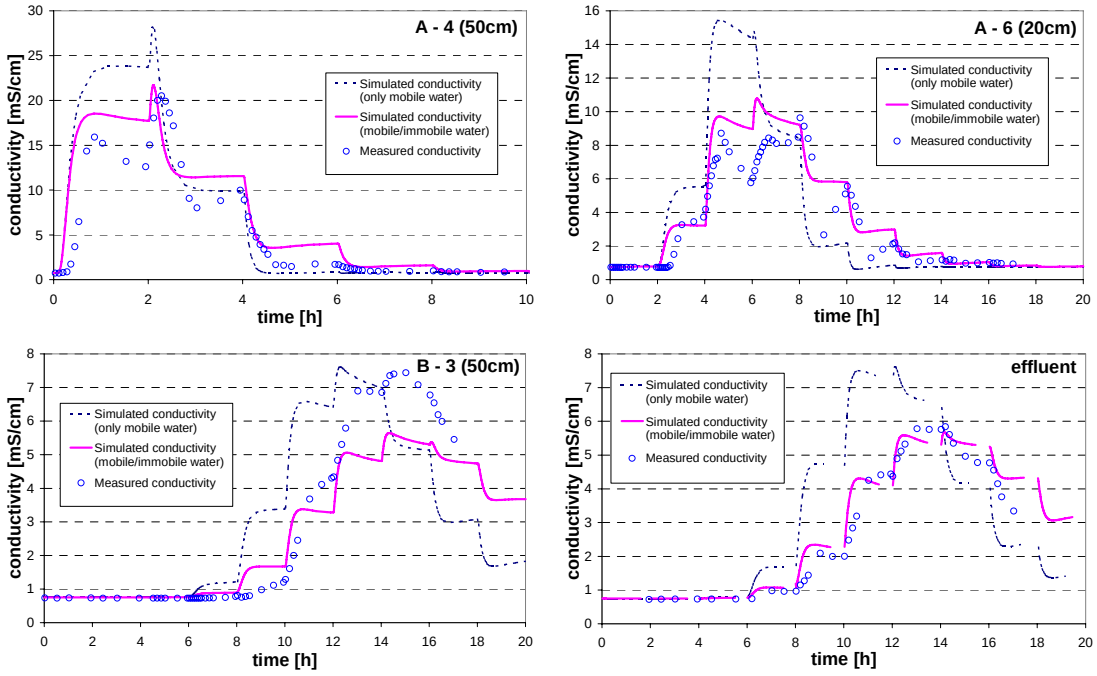

Figure 5.18: Simulated and measured electrical conductivities for three sampling points and at the outlet (Langergraber, 2003).

Simulation of multi-component reactive transport

Table 5.9 shows the influent concentrations for the multi-component reactive transport simulations. Since this system was used to treat polluted surface water, the concentrations are much lower compared to wastewater.

Table 5.9. Influent concentrations for the multi-component reactive transport simulations.

Parameter	**O2**	**CR**	**CS**	**CI**	**NH4N**	**NO2N**	**NO3N**	**N2N**	**IP**
Value	1	15	1	1	6.5	0.1	2	10	0.4

Figure 5.19 shows the distribution of heterotrophic organisms XH. The maximum XH concentration is in the upper part of the main layer of the downflow chamber. Bacteria concentrations decrease with depth. In the upflow chamber the bacteria concentration is low because of a lack of substrate.

Figure 5.20 shows the distribution of *Nitrosomonas* XANs. The distribution of the second autotrophic organism, *Nitrobacter* XANb, was found to be very similar (not further shown here). Again, most autotrophic bacteria were located in the upper part of the downflow chamber. The maximum concentration of autotrophic bacteria was lower than the maximum concentration of the heterotrophic bacteria. The concentration decreased faster with the depth for the autotrophic bacteria than for the heterotrophic bacteria. This is a direct consequence of nitrification being a strictly aerobic process, with oxygen being only available in the upper parts of the downflow chamber (see also Figure 5.21).

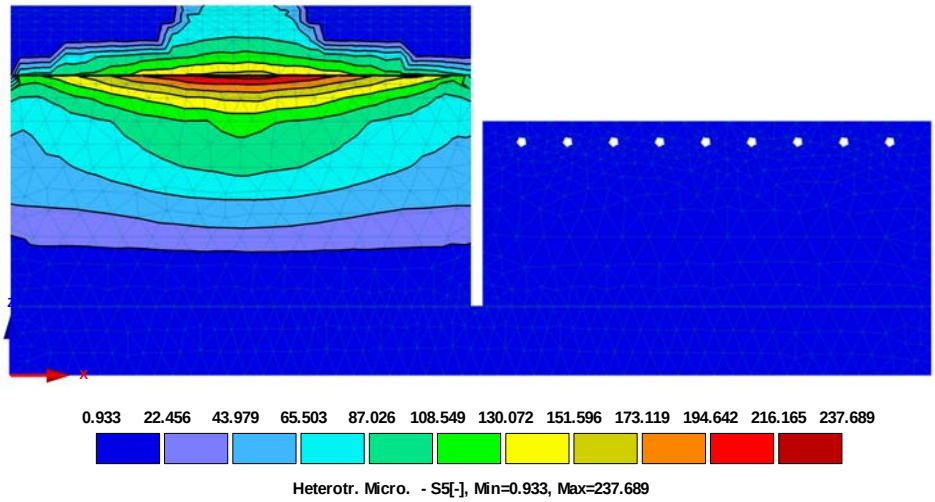

Figure 5.19: Simulated steady-state distribution of heterotrophic organisms XH.

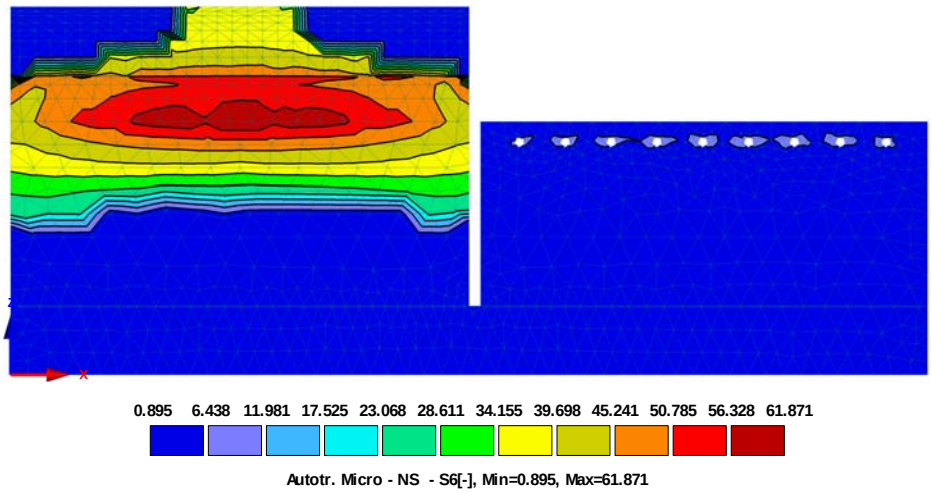

Figure 5.20: Calculated steady-state distribution of *Nitrosomonas* XANs.

Figure 5.21 shows time series of dissolved oxygen for two consecutive applications to the main layer in the downflow chamber (0 cm) and at two different depths (5 cm and 15 cm, located in the unsaturated and saturated zones, respectively). After loading, the DO concentration decreases at the surface and at the 5 cm depth. At 15 cm depth, however, the DO concentration increases due to advective DO transport with the infiltrating water. Still, oxygen decreased quickly (within 15 minutes after loading) due to the consumption of oxygen. No oxygen was found at 15 cm depth (i.e., in the saturated zone) during the remainder of the simulation. In the unsaturated zone (5 cm depth) the DO concentration increases again due to re-aeration, and reaching oxygen saturation after about 1 hour after loading.

Figure 5.22 shows time series of ammonium and nitrate nitrogen at the surface of the main layer (0 cm) and at three different depths (5 cm, located in the unsaturated zone, and 15 cm and 30 cm, located in the saturated zone). After loading, NH4N increases whereas NO3N decreases. Further on NH4N is nitrified resulting in an increasing NO3N concentration. At 15 cm depth changes in concentration occur mainly due to convection since oxygen is already a limiting factor (Figure 5.21). Notice, again, that only small changes in concentrations occur at 30 cm depth.

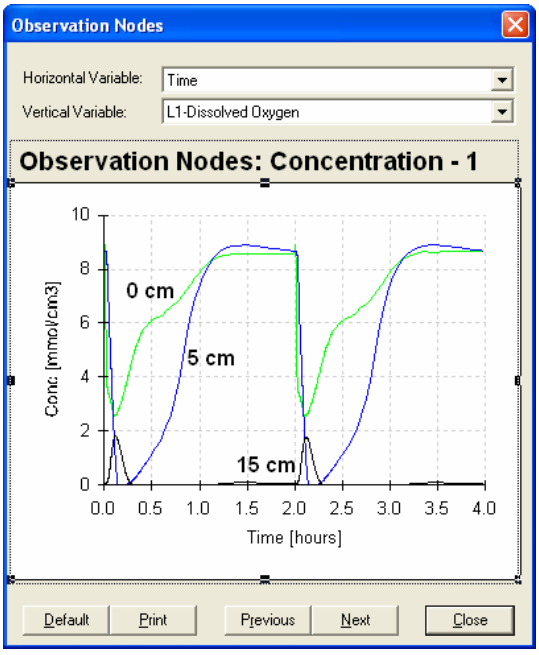

Figure 5.21: Simulated time series of dissolved oxygen.

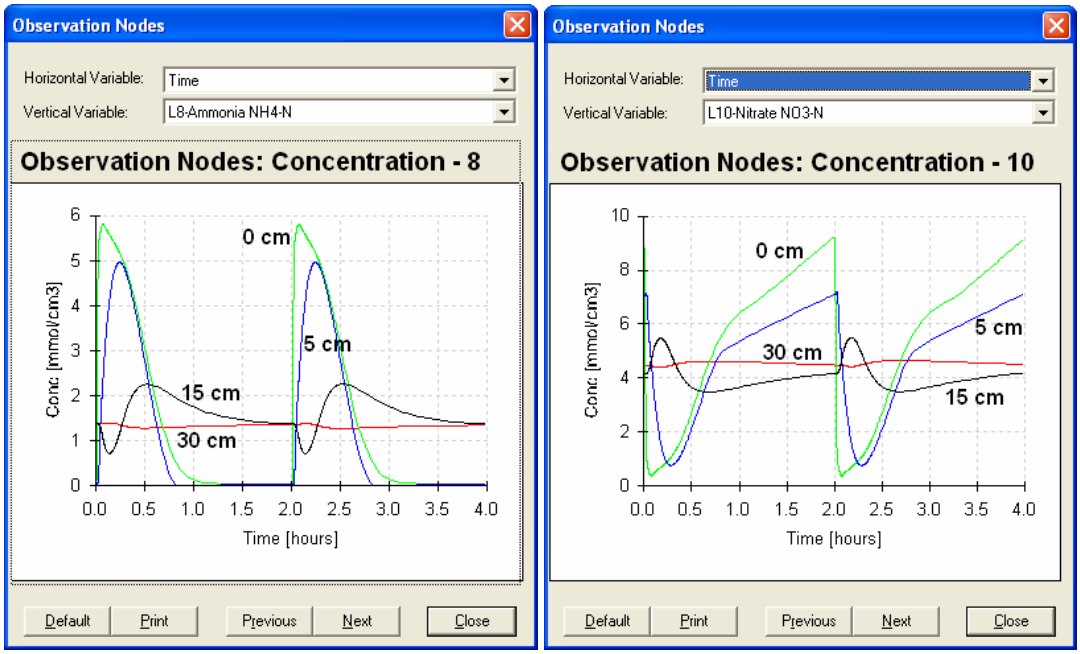

Figure 5.22: Simulated time series of ammonium nitrogen (left) and nitrate nitrogen (right).

5.3 Constructed wetland for treatment of combined sewer overflow

5.3.1 System description

CW2D was tested to model a subsurface flow constructed wetland for the treatment of combined sewer overflow (CSO). CWs for the treatment of CSO are generally designed as vertical flow soil filters with a detention basin on top of the filter layer. Main treatment objectives are (1) detention and reduction of peak flows, (2) reduction of suspended solids by filtration and (3) reduction of soluble and particulate pollutants by adsorption and subsequent biological degradation (Dittmer et al., 2005). To reach the first objective throttle valves are applied to limit the maximum effluent flow rate and therefore the flow velocity in the filter itself. For simulation purposes the maximum allowed effluent flow rate had to be implemented.

Fundamental differences between wetlands for wastewater and CSO treatments are the loading regime and the quality parameters of the inflow. In the CSO treatment the succession of loading events and dry periods is characterized by the stochastic nature of rainfall and the runoff behaviour of the catchment area. Extreme cases involve a permanent loading for weeks on the one hand, and several months without any loading event on the other. Loading rates (inflow/filter area) show a high variability ranging from mean values of 0.02 mm/s for less intensive rain events, up to peak flows of 1 mm/s during intensive storm events.

Quality parameters of CSO show generally lower pollution than wastewater. Organic matter predominantly occurs in particulate form, which can mainly be attributed to remobilisation of sewer sediments. As this effect is strongly related to the flow rate, total suspended solid concentrations, as well as solute/particulate ratio of pollutants, are highly variable within the course of a rain event.

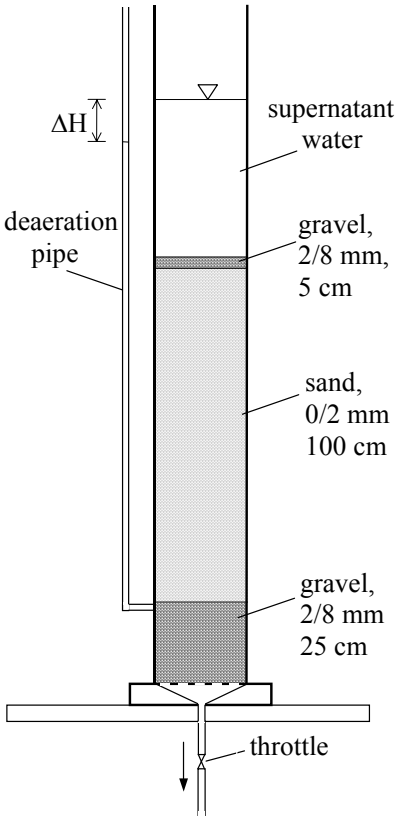

Figure 5.23: Lab-scale filter column.

Simulations were performed for a lab-scale column (diameter 19 cm, Figure 5.23). The laboratory layout corresponds to the layering of a full scale CW. The main layer consists of sand (grain size 0/2 mm, effective size 0.1 mm, coefficient of uniformity 2.8). The upper gravel layer serves to prevent erosion, while the gravel layer below the filter represents the drainage system.

The test site consists of 6 columns, which are all fed identically. The filtration rate of columns 1 to 4 is manually controlled by a throttle in the outlet; Columns 5 and 6 have a free drainage (Table 5.10).

Table 5.10: Drainage regime of the filter columns.

Column	C 1/2	C 3/4	C 5/6
Drainage	throttled	throttled	free
Filtration rate (m/h)	0.036	0.180	-
Effluent flow (litre/h)	1	5	-

The columns are loaded regularly once a week with 15.7 litres of synthetic sewer, which corresponds to a loading rate of 0.5 m/event. The entire volume is applied within about 3 minutes. During infiltration the level of the supernatant water, the water level in the deaeration pipe and the effluent flow rate are measured (variable time steps 30 sec to 30 min). The synthetic sewer is based on the OECD guideline 303A (OECD, 1981), but is diluted to obtain concentrations within the range of CSO quality parameters.

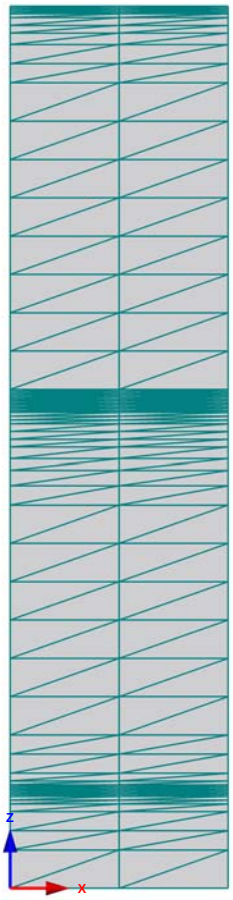

Figure 5.24: Two-dimensional finite element mesh of the lab-scale column.

Tracer experiments using potassium bromide (KBr) were carried out. The loading procedure was divided into three steps. The columns were first loaded with 9.5 litres of bromide-free water, and after this volume has infiltrated, another 2.5 litres were applied containing 10 mg/l Br^-. Finally after the tracer has infiltrated, the last 3.5 litres of bromide-free were loaded. Br^- concentrations in the effluent were measured with an ion-selective electrode.

5.3.2 Simulation set up

For the simulation a structured two-dimensional finite element mesh with 105 rows and 3 columns resulting in 315 nodes and 416 elements was used (Figure 5.24). An atmospheric boundary condition was applied on top of the upper layer, while a free drainage or seepage face with maximum allowed flux was used at the bottom.

The supernatant water level decreases from about 40 to 45 cm immediately after the loading with a rate of 2.5 cm/minute. To simulate this behaviour a "virtual" layer with 100 % pore volume was used at the top (Dittmer et al., 2005).

5.3.3 Simulation results

Calibration of Flow and Transport Models

CW2D has successfully been applied to model wetlands with free drainage. CWs for CSO treatment are generally operated with a controlled effluent flow rate. As loading rates and intervals are determined by rainfall, operation of the effluent throttle is the only way to influence the performance of the plant. It is therefore essential that the model gives correct results for a wide span of possible effluent flow rates. Hence, the flow model was calibrated on the basis of data obtained from operation with free drainage. The calibrated model was than applied to the columns with controlled effluent rates (Dittmer et al., 2004).

The retention and hydraulic conductivity functions for unsaturated conditions were modelled using the van Genuchten-Mualem equations (van Genuchten, 1980) implemented in HYDRUS-2D. Values for the sand (gravel) layer are given in Table 5.11 (Dittmer et al.,

2005). The virtual layer for supernatant water was simulated with $\theta_r = 0$ and $\theta_s = 1$ and $K_s = 10^6$ cm/h. With these values, head loss and retardation within this layer are negligible. The longitudinal dispersivity used was 2 cm in the top layer and 3 cm_s in the other layers, the transverse dispersivity used was 10 cm_s for all layers.

Table 5.11: Values of the van Genuchten model parameters.

Parameter	**Depth**	**Residual water content θ_r**	**Saturated water content θ_s**	**Parameters** α	n	**Saturated hydraulic conductivity K_s**
Unit	(cm)	(cm_w^3 / cm_s^3)	(cm_w^3 / cm_s^3)	(cm_s^{-1})	(-)	(cm/h)
1) Top layer	100	0	1	0.35	3	1000000
2) Gravel	5	0.05	0.37	0.05	2. 8	36000
3) Main layer	100	0.055	0.30	0.02	3	1000
4) Gravel	25	0.05	0.37	0.05	2.8	36000

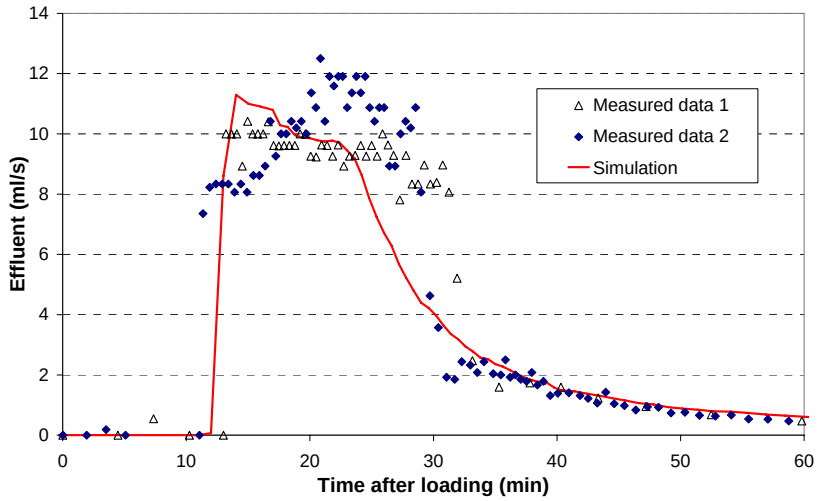

Figure 5.25: Measured and simulated effluent flow rate of column 6.

Figure 5.25 and Figure 5.26 show the measured and simulated effluent flow rates and tracer breakthrough curves for column 6, respectively. Several measured curves of effluent rates in Figure 5.25 show significant variations that occurred despite virtually identical conditions of all loading events. This confirms that the infiltration process under the given combination of basic conditions (free drainage, extremely high loading rate and pressure head of supernatant water) is extremely sensitive. Considering these uncertainties simulated and measured data show a good match.

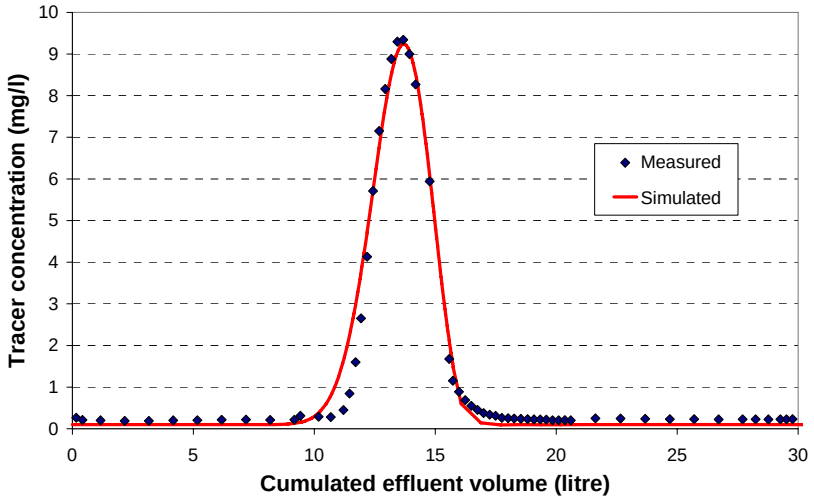

Figure 5.26: Measured and simulated breakthrough curves of column 6.

Simulation with controlled flow rate

As described above the operation of a constructed wetland for CSO treatment is generally with a controlled flow rate. This was implemented by setting a maximum for a seepage face flux. This option, i.e., the maximum allowed flux at the seepage face, is initiated by setting the logical variable lSeepLimit to true in the `"options.in"` input file (see description in Chapter 6.2).

Parameters obtained above were used for simulation runs with the controlled flow rate. The throttle has no influence on the infiltration rate (gradient of supernatant water level) at the beginning. When the soil becomes largely saturated after about 11 minutes, the simulated infiltration rate abruptly drops to the level of the effluent rate. In the laboratory experiment this decrease took about another 10 minutes. The final level of saturation is not reached instantaneously. This difference can be explained by the influence of air flow within the columns, which is not considered in the model.

Figure 5.27 shows results of simulations for the lab-scale columns with free drainage and controlled effluent flow rates, respectively. The settings for the controlled effluent rate case: qSLimit = 3.6 cm/h (the maximum allowed flow rate, corresponding to 68.4 cm²/h or 1 litre/hour) and hSeep = -100 cm (the maximum allowed pressure head). Note that while the left graph in Figure 5.27 uses minutes as time units, the right graph uses hours. While in the flow unrestricted case the bulk of water passed through the CW system in only about 1 hour, in the flow restricted case this happened in about 17 hours. Obviously, in the flow restricted case, the water and dissolved pollutants had much longer contact with the gravel material.

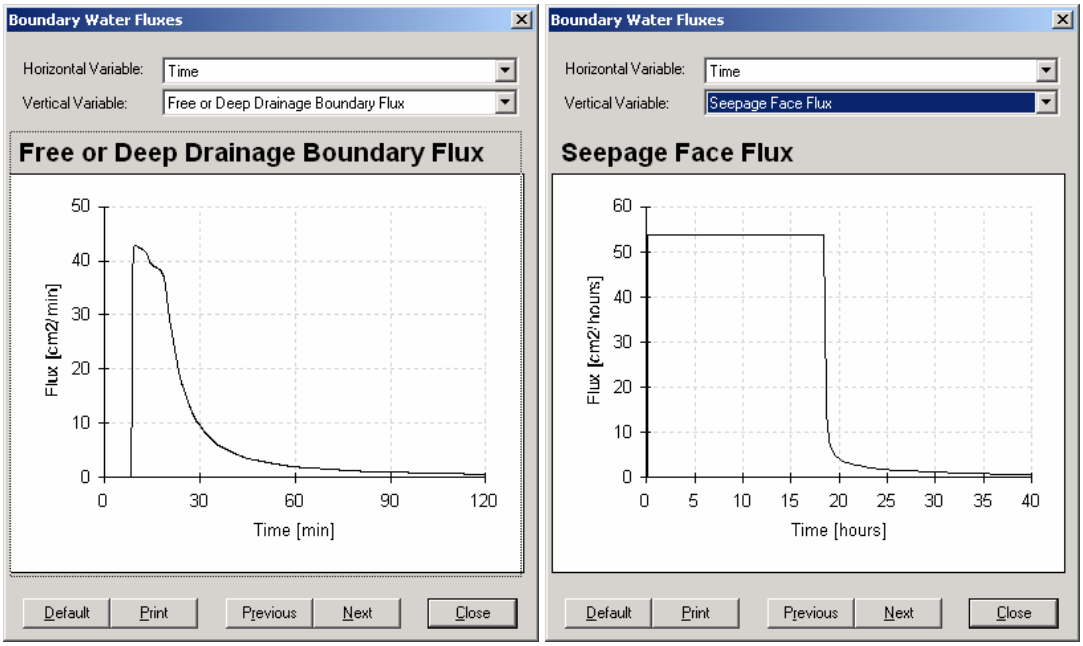

Figure 5.27: Comparison of simulations with free drainage BC (time units = minutes) and limited seepage face flux (time units = hours).

Figure 5.28 shows measured and simulated breakthrough curves of column 4 and column 2 with controlled effluent rates 5 litres/hour and 1 litre/hour, respectively. Using the transport parameters obtained from the free drainage simulations (column 6) the tracer experiments with controlled effluent rate could be simulated.

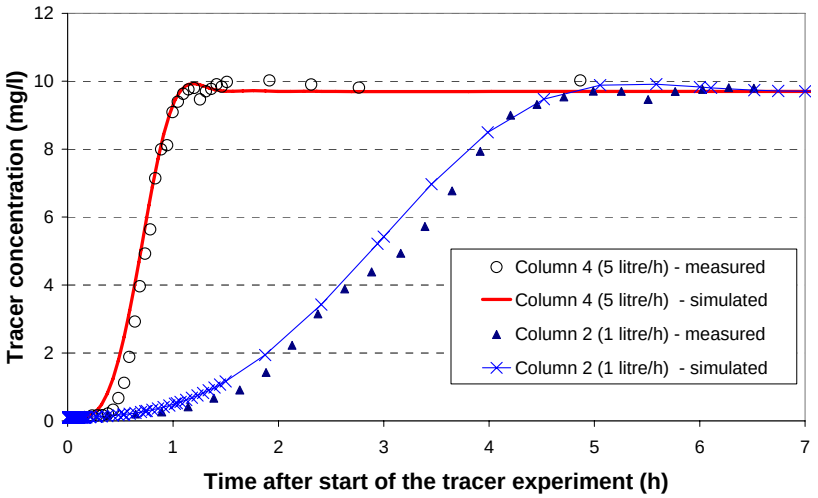

Figure 5.28: Measured and simulated breakthrough curves of column 4 and column 2 (controlled effluent rate 5 litre/hour and 1 litre/hour, respectively).

5.4 Experiences, limitations and research need

Our simulation results showed a good match with the measured data for both single- and multi-component reactive transport when the hydraulic behaviour of the system was accurately described. The importance of the water flow model was evident from a sensitivity analysis that showed that results of the reactive transport simulations were very sensitive to model parameters describing the unsaturated properties of the substrate. The good match of the experimental data with the reactive transport simulations could be obtained using literature values for the CW2D model parameters (Langergraber, 2001).

The CW2D module at present considers the main constituents of domestic wastewater. Therefore, CW2D is only applicable to constructed wetlands that treat domestic wastewater or waters with properties that can be described with parameters currently incorporated into CW2D. If other components and/or waters are to be modelled, extensions to the present model will be needed.

Further limitations of CW2D result from assumptions of the basic model, the Activated Sludge Model (ASM). These include consideration of: a) a constant value of pH, b) constant coefficients in the rate equations, c) constant stoichiometric factors, and d) a limited temperature range from 10°C to 25°C (Henze et al., 2000).

Although simulations showed a good match with the measured data, much research remains so as to produce a reliable tool for constructed wetland design. The main research needs regarding modelling of constructed wetland processes as listed by Langergraber (2003) are:

1. *Detailed hydraulic investigations of full-scale constructed wetlands*: A good match between simulation results and measured data can be obtained when sufficient data are available to describe the hydraulic behaviour of the system and thus when the flow model can be successfully calibrated. For full-scale systems, the match between the model and data was relatively poor thus far, most probably due to a lack of data to accurately describe the hydraulic behaviour of the system (Langergraber, 2001) and due to the inherent heterogeneity of large-scale systems. The heterogeneity of the substrate and uneven distribution of influent water on the surface are the main reasons for needing detailed hydraulic investigations of full-scale systems.
2. *Numerical simulations of outdoor constructed wetland systems*: Simulations of outdoor (full-scale) constructed wetland systems are also needed to validate the temperature dependencies of various processes considered in CW2D. It has been shown that by introducing temperature dependencies for the half-saturation constants of hydrolysis and nitrification it is possible to simulate the effluent concentrations at low temperatures (Langergraber, 2005b). Temperature dependency for these kinetic parameters (K_X and $K_{ANs,NH4}$) has been considered also by other authors (e.g. Bornemann et al., 1998).
3. *Investigation of plant uptake models*: Models describing nutrient (nitrogen and phosphorus) uptake by plants have to be considered in order to describe the contribution of plants to the overall treatment process. Langergraber (2005a) showed the important influence of plant uptake on effluent concentrations and removal efficiency using plant uptake models that are currently available in HYDRUS-2D (Šimůnek et al., 1999). These models describe nutrient uptake associated with water uptake (i.e., active uptake). For wastewater the simulated plant uptake matched the potential uptake that was calculated using literature values. In the less loaded systems

(lower nutrient concentrations in the influent water) the concentrations of nitrogen and phosphorus in the liquid phase are too low to reach the potential uptake rates.

It can be said that it is possible to simulate plant uptake in subsurface flow constructed wetlands using a model that describes nutrient uptake coupled to water uptake. For high loaded systems the model gives good results, whereas for waters with lower nutrient contents the simulation results indicate that potential nutrient uptake will be substantially overestimated when using literature values to calculate the potential uptake, compared to simulations using models that couples nutrient uptake to water uptake.

4. *Need for a module describing substrate clogging*: One limitation of CW2D is that up to now only dissolved solutes are being considered. Wastewater often contains suspended solids that may cause pore clogging. Clogging is considered to be the biggest operational problem affecting vertical flow in constructed wetlands. It causes a reduction in the infiltration capacity of the substrate surface, and therefore often a rapid decline in the treatment performance of the system (e.g., Platzer and Mauch, 1997, Winter and Goetz, 2003, Langergraber et al., 2003). The clogging module should be able to describe pore size reductions due to the settling of suspended solids and due to bacteria growth. Both particle transport and bacteria growth models are currently available (e.g., Mackie & Bai, 1993; Vandeviere et al., 1995; Kildsgaard & Engesgaard, 2001) and could be incorporated into CW2D/HYDRUS. The effects of pore size reduction on the hydraulic properties of the substrate may also need to be taken into account (e.g., Taylor & Jaffé, 1990; Magnico, 2000).
5. *Improved experimental methods for estimating CW2D model parameters*: There is also a need for improved technologies to measure CW2D model parameters of the reactive transport part of the model. This is important before the model can be used as a design tool. A number of measurement techniques have been developed to characterise the parameters of Activated Sludge Models as applied to activated sludge wastewater treatment plants (Henze et al., 2000; Vanrolleghem et al., 1999). However, no experimental techniques are currently available to measure CW2D model parameters. Detailed investigations on microbial biocoenosis in particular must be carried out, with a need to adapt existing measurement methods to soil and/or wastewater environments. The Austrian research project "*Characterisation of microbial biocoenosis to optimise removal efficiency and design of subsurface flow constructed wetlands for wastewater* treatment", funded by the Austrian Science Fund (FWF, project No. P16212-B06, duration 05/2003-04/2006), targets this problem (Tietz et al., 2005).

5.5 Possible future applications

CW2D was developed to model subsurface flow constructed wetlands for wastewater treatment. However, it was already successful applied also to model constructed wetlands for the treatment of combined sewer overflows (see Chapter 5.3). Possible future applications could include:

- Constructed wetlands for other types of wastewater, such as industrial and agricultural wastewaters with a composition similar to municipal wastewater.
- Infiltration of treated (waste)water into soil for e.g. groundwater recharge
- Carbon and nitrogen cycling in soils
- Processes in natural wetlands
- Processes in riparian areas

6 Input data

6.1 Extension of the 'selector.in' input file to enter parameters defined in CW2D

At its end the file 'selector.in' includes the additional block containing parameters defined in CW2D (BLOCK_X see below). These parameters include kinetic parameters and their temperature dependencies, stoichiometric parameters, and parameters for the model of oxygen re-aeration. The kinetic parameters are described in Table 6.1 (see also Table 3.8), the stoichiometric and composition parameters, and parameters for the model of oxygen re-aeration in Table 6.2 (see also Table 3.5 and Table 3.4).

```
*** BLOCK_X:_parameters_for_biokinetic_model **********************
Hydrolysis
    Kh_20_[1/d]   KX_20
         3.0        0.1
Heterotrophic organisms: Mineralisation
   mueHet_20    bHet_20   KHet_O2_20  KHet_CR_20 KHet_NH4_20 KHet_IP_20  [g/m3]
         6.0        0.4          0.2           2        0.05       0.01
Heterotrophic organisms: Denitrification
    mueDN_20  KDN_O2_20   KDN_NO3_20  KDN_NO2_20   KDN_CR_20 KDN_NH4_20 KDN_IP_20
         4.8        0.2          0.5         0.5           2       0.05      0.01
Autotrophic bacteria: Nitrosomonas
   mueANs_20    bANs_20   KANs_O2_20 KANs_NH4_20  KANs_IP_20
         0.9       0.15            1         0.5        0.01
Autotrophic bacteria: Nitrobacter
   mueANb_20    bANb_20   KANb_O2_20 KANb_NO2_20 KANb_NH4_20 KANb_IP_20
         1.0       0.15          0.1         0.1        0.05       0.01
Temperature dependency (activation_energy [J/mol] for Arrhenius equation)
    Tdep_het   Tdep_aut      Tdep_Kh     Tdep_KX
       47800      69000        28000      -53000

Stoichiometric_parameters
 f_Hyd_CI f_BM_CR f_BM_CI [gCOD/gCOD]
 0.       0.1     0.02
 Y_Het_[gCOD(BM)/gCOD(CR)]  Y_ANs_[gCOD(BM)/gNH4N]  Y_ANb_[gCOD(BM)/gNO2N]
 0.65                       0.24                    0.24
 iN_CR iN_CS iN_CI iN_BM [gN/gCOD]
 0.03  0.04  0.01  0.07
 iP_CR iP_CS iP_CI iP_BM [gP/gCOD]
 0.01  0.01  0.01  0.02

Oxygen
 cO2_sat_20_[mg/l] Tdep_cO2_sat_[J/mol] rate_O2_[1/d]
 9.18              -15000               240.0
*****************************************************************
```

Table 6.1: Description of variables of "BLOCK X" in the `'selector.in'` input file – Part 1: kinetic parameters.

Variable name	Type	Unit	Default	Description
Hydrolysis				
Kh_20	float	[1/d]	3.00	hydrolysis rate constant
KX_20	float	[g/m³]	0.10	sat./inh. coeff. for hydrolysis
Heterotrophic organisms 1: Mineralisation				
mueHet_20	float	[1/d]	6.00	maximum aerobic growth rate on CR
bHet_20	float	[1/d]	0.40	rate constant for lysis
KHet_O2_20	float	[g/m³]	0.20	saturation/inhibition coefficient for O2
KHet_CR_20	float	[g/m³]	2.00	saturation/inhibition coeff. for substrate
KHet_NH4_20	float	[g/m³]	0.05	saturation/inhibition coeff. for NH4 (nutrient)
KHet_IP_20	float	[g/m³]	0.01	saturation/inhibition coeff. for P
Heterotrophic organisms 2: Denitrification				
mueDN_20	float	[1/d]	4.80	maximum denitrification rate
KDN_O2_20	float	[g/m³]	0.20	saturation/inhibition coeff. for O2
KDN_NO3_20	float	[g/m³]	0.50	saturation/inhibition coeff. for NO3
KDN_NO2_20	float	[g/m³]	0.50	saturation/inhibition coeff. for NO2
KDN_CR_20	float	[g/m³]	2.00	saturation/inhibition coeff. for substrate
KDN_NH4_20	float	[g/m³]	0.05	saturation/inhibition coeff. for NH4 (nutrient)
KDN_IP_20	float	[g/m³]	0.01	saturation/inhibition coeff. for P
Autotrophic bacteria 1: Nitrosomonas				
mueANs_20	float	[1/d]	0.90	maximum aerobic growth rate on NH4N
bANs_20	float	[1/d]	0.15	rate constant for lysis
KANs_O2_20	float	[g/m³]	1.00	saturation/inhibition coeff. for O2
KANs_NH4_20	float	[g/m³]	0.05	saturation/inhibition coeff. for NH4
KANs_IP_20	float	[g/m³]	0.01	saturation/inhibition coeff. for P
Autotrophic bacteria 2: Nitrobacter				
mueANb_20	float	[1/d]	1.00	maximum aerobic growth rate on NO2N
bANb_20	float	[1/d]	0.15	rate constant for lysis
KANb_O2_20	float	[g/m³]	0.10	saturation/inhibition coeff. for O2
KANb_NO2_20	float	[g/m³]	0.10	saturation/inhibition coeff. for NO2
KANb_NH4_20	float	[g/m³]	0.05	saturation/inhibition coeff. for NH4 (nutrient)
KANb_IP_20	float	[g/m³]	0.01	saturation/inhibition coeff. for P
Temperature dependency (activation energy for Arrhenius equation)				
Tdep_het	float	[J/mol]	47'800	activation energy for heterotrophic bacteria
Tdep_aut	float	[J/mol]	69'000	activation energy for autotrophic bacteria
Tdep_Kh	float	[J/mol]	28'000	activation energy for hydrolysis rate
Tdep_KX	float	[J/mol]	-53'000	activation energy for KX

Table 6.2: Description of variables of "BLOCK X" in the `'selector.in'` input file – Part 2: stoichiometric and composition parameters, and parameters for the model of oxygen re-aeration.

Variable name	Type	Unit	Default	Description
Stoichiometric and composition parameters				
f_Hyd_CI	float	[gCOD/gCOD]	0.00	production of CI in hydrolysis
f_BM_CR	float	[gCOD/gCOD]	0.10	fraction of CR generated in biomass lysis
f_BM_CI	float	[gCOD/gCOD]	0.02	fraction of CI generated in biomass lysis
Y_Het	float	[gCOD(BM)/gCOD(CR)]	0.65	yield coefficient for heterotrophs
Y_ANs	float	[gCOD(BM)/gNH4N]	0.24	yield coefficient for *N.somonas*
Y_ANb	float	[gCOD(BM)/gNO2N]	0.24	yield coefficient for *N.bacter*
iN_CR	float	[gN/gCOD]	0.03	N content of CR
iN_CS	float	[gN/gCOD]	0.04	N content of CS
iN_CI	float	[gN/gCOD]	0.01	N content of CI
iN_BM	float	[gN/gCOD]	0.07	N content of biomass
iP_CR	float	[gP/gCOD]	0.01	P content of CR
iP_CS	float	[gP/gCOD]	0.01	P content of CS
iP_CI	float	[gP/gCOD]	0.01	P content of CI
iP_BM	float	[gP/gCOD]	0.02	P content of biomass
Oxygen				
cO2_sat_20	float	[g/m³]	9.18	saturation concentration of oxygen
Tdep_cO2_sat	float	[J/mol]	-15000	activation energy for saturation concentration of oxygen
rate_O2	float	[1/d]	240	re-aeration rate

6.2 The 'options.in' input file

Two additional options, namely limited effluent flow rates and assignment of temperature dependency for the saturation/inhibition coefficient for NH4 in the first step of nitrification as described by Langergraber (2005b), can be specified in the additional input file 'options.in'. The third additional option, personalized print intervals for the simulation results, is only needed for the HYDRUS-2D software package whereas this feature is already supported by the HYDRUS graphical user interface.

The 'options.in' input file is not supported by the graphical user interface of the HYDRUS software. It needs to be created manually and placed in the temporary working directory created by HYDRUS (Šimůnek et al., 2006a). If this input file does not exist, CW2D/HYDRUS considers its default values.

The definition of variables used in 'options.in' is given in Table 6.3, and an example of the file is given below:

```
Input file "Options.in"
hSeep [L]  lSeepLimit   qSLimit (positive)
0.         f            0.
Tdep_KANs_NH4 [J/mol]
0.
lPrintD      tPrintInt [T]        nPrintInt [time steps]
t            0.05                 20
```

Table 6.3: Description of variables used in the 'options.in' input file.

Variable name	Type	Unit	Description
hSeep	float	[L]	Maximum allowed seepage face pressure head If the pressure head exceeds the hSeep value, the seepage face flux is limited to qSLimit
lSeepLimit	logical	-	= true: use the maximum effluent flow rate for a seepage face BC; = false: normal seepage face BC
qSLimit	float	[L/T]	Maximum allowed seepage face flux (positive)
Tdep_KANs_NH4	float	[J/mol]	= activation energy for saturation/inhibition coeff. for NH4 in the first step of nitrification (Tdep_KANs_NH4 = -160'000 J/mol; Langergraber, 2005b)
lPrintD	logical	-	= true: print results at the specified time interval = false: normal print
tPrintInt	float	[T]	Print results after every tPrintInt time interval
nPrintInt	integer	[time steps]	Print results after every nPrintInt time steps

7 Output data

7.1 Format of the 'effluent.out' output file

An additional output-file 'effluent.out' is created that contains information about effluent concentrations along the outflow boundary. If multiple outflow boundaries exist, only the concentration value for the first boundary from this list (free drainage boundary, seepage face boundary, variable flux boundary, and constant flux boundary) is printed. This file is printed during the simulation run.

```
All solute fluxes and cumulative solute fluxes are positive out of the region

      Time       cEff(1)       cEff(2)     ...   cEff(12)      cEff(13)     TempEff

     .0000010   .870194E+01   .227306E+00  ...  .162806E+01   .138496E+01     20.0000
     .0009541   .870195E+01   .227296E+00  ...  .162805E+01   .138496E+01     20.0000
     .0033000   .870198E+01   .227269E+00  ...  .162804E+01   .138496E+01     20.0000
     :
     :
```

The 'effluent.out' output file can be found in the temporary working directory created by HYDRUS (Šimůnek et al., 2006a).

8 List of examples

a) Wetland1

Pilot-scale vertical flow constructed wetland (PSCW, chapter 5.1) for flow and reactive transport simulations.

b) Wetland2

Two-stage vertical flow constructed wetland (SSP, chapter 5.2) for reactive transport simulation.

c) Wetland3

Lab-scale vertical flow constructed wetland for treatment of combined sewer overflow (CSOCW, chapter 5.3) as an example for controlled effluent rate.

9 References

[1] Antonopoulos, V.Z., Wyseure, G.C.L. (1998): Modeling of water and nitrogen dynamics on an undisturbed soil and a restored soil after open-cast mining. *Agricultural Water Management* 37, 21-40.

[2] Birkinshaw, S.J., Ewen, J. (2000): Nitrogen transformation component for SHETRAN catchment nitrate transport modeling. *Journal of Hydrology* 230, 1-17.

[3] Bolton, K.G.E., Greenway, M. (1999): Nutrient sinks in a constructed *melaleuca* wetland receiving secondary treated effluent. *Water Science & Technology* 40(3), 341-347.

[4] Bornemann, C., Londong, J., Freund, M., Nowak, O., Otterpohl, R., Rolfs, T. (1998): Hinweise zur dynamischen Simulation von Belebungsanlagen mit dem Belebtschlammodell Nr.1 der IAWQ. *Korrespondenz Abwasser* KA 45(3), 455–462 [*in German*].

[5] Bouwer, E.J., Cobb, G.D. (1987): Modeling of biological processes in the subsurface. *Water Science & Technology* 19, pp.769-779.

[6] Brouwer, H., Klapwijk, A., Keesman, K.J. (1998): Identification of activated sludge and wastewater characteristics using respirometric batch-experiments. *Water Research* 32(4), 1240-1254.

[7] Chung, S.-O., Horton R. (1987): Soil heat and water flow with a partial surface mulch. *Water Resources Research 23*(12), 2175-2186.

[8] DeSimeone, L.A., Howes, B.L. (1998): Nitrogen transport and transformations in a shallow aquifer receiving wastewater discharge: A mass balance approach. *Water Resources Research* 34(2); 271-285.

[9] Dittmer, U., Meyer, D., Langergraber, G. (2005): Simulation of a Subsurface Vertical Flow Constructed Wetland for CSO Treatment. *Water Science & Technology* 51(9), 225-232.

[10] Gray, S., Kinross, J., Read, P., Marland, A. (2000): The nutrient capacity of mearl as a substrate in constructed wetland systems for wastewater treatment. *Water Research* 34(8), 2183-2190.

[11] Grosse, W., Wissing, F., Perfler, R., Wu, Z., Chang, J., Lei, Z. (1999): Biotechnological approach to water quality improvement in tropical and subtropical areas for reuse and rehabilitation of aquatic ecosystems. Final report, INCO-DC Project Contract n°ERBIC18CT960059, Cologne, Germany.

[12] Gujer, W., Henze, M., Mino, T., van Loosdrecht, M.C.M. (1999): Activated Sludge Model No.3. *Water Science & Technology* 39(1), 183–193.

[13] Haberl, R., Grego, S., Langergraber, G., Kadlec, R.H., Cicalini, A.R., Martins Dias, S., Novais, J.M., Aubert, S., Gerth, A., Thomas, H., Hebner, A. (2003): Constructed wetlands for the treatment of organic pollutants. *JSS - J Soils & Sediments* 3(2), 109-124.

[14] Henze M., Grady, Jr. C.P.L., Gujer, W., Marais, G.v.R., Matsuo, T. (1987): Activated Sludge Model No.1. *IAWPRC Scientific and Technical Report No.1*, IAWPRC, London, UK.

[15] Henze, M., Gujer, W., Mino, T., Matsuo, T., Wentzel,M.C., Marais, G.v.R. (1995): Activated Sludge Model No.2. *IAWQ Scientific and Technical Report No.3*, IAWQ, London, UK.

[16] Henze, M., Gujer, W., Mino, T. Matsuo, T., Wentzel,M.C., Marais, G.v.R., van Loosdrecht, M.C.M. (1999): Activated Sludge Model No.2D (ASM2D). *Water Science & Technology* 39(1), 165-182.

[17] Henze, M., Gujer, W., Mino, T., van Loosdrecht, M.C.M. (2000). Activated sludge models ASM1, ASM2, ASM2D and ASM3. *IWA Scientific and Technical Report No.9*, IWA Publishing, London, UK.

[18] Horn, H., Hempel, D.C. (1998): Modeling mass transfer and substrate utilization in the boundary layer of biofilm systems. *Water Science and Technology* 37(4-5), 139-147

[19] Jacob, J., Le Lann, J.-M., Pingaud, H., Capdeville, B. (1997): A generalized approach for dynamic modelling and simulation of biofilters: application to wastewater denitrification. *Chemical Engineering Journal* 65, 133-143.

[20] Kadlec, R.H. (2000): The inadequacy of first-order treatment kinetic models. *Ecological Engineering* 15, 105–119.

[21] Kadlec, R.H., Knight, R.L. (1996): *Treatment wetlands*. CRC Press, Boca Raton, FL, USA.

[22] Kadlec, R.H., Knight, R.L., Vymazal, J., Brix, H., Cooper, P., Haberl, R. (eds, 2000): Constructed wetlands for pollution control – Processes, performance, design and operation. *IWA Scientific and Technical Report No.8*. IWA Publishing, London, UK.

[23] Kaluarachchi, J.J., Parker, J.C. (1988): Finite element model of nitrogen species transformation in the unsaturated zone. *Journal of Hydrology* 103(3-4), 249-274.

[24] Karpiscak, M.M., Freitas, R.J., Gerba, C.P., Sanchez, L.R., Shamir, E. (1999): Management of diary waste in the Sonoran Desert using constructed wetland technology. *Water Science & Technology* 40(3), 57-65.

[25] Kildsgaard, J., Engesgaard, P. (2001): Numerical analysis of biological clogging in two-dimensional sand box experiments. *Journal of Contaminant Hydrology* 50, 261-285.

[26] Langergraber, G. (2001): Development of a simulation tool for subsurface flow constructed wetlands. *Wiener Mitteilungen* 169, Vienna, Austria, 207p, ISBN 3-85234-060-8.

[27] Langergraber, G. (2003): Simulation of subsurface flow constructed wetlands - Results and further research needs. *Water Science & Technology* 48(5), 157-166.

[28] Langergraber, G. (2005a): The role of plant uptake on the removal of organic matter and nutrients in subsurface flow constructed wetlands – A simulation study. *Water Science & Technology* 51(9), 213-223.

[29] Langergraber, G. (2005b): Simulation of the treatment performance of outdoor subsurface flow constructed wetlands in temperate climates. In: De Pauw, N., Tack, F. (eds.): *International Symposium on "Wetland Pollutant Dynamics and Control – WETPOL" – Book of Abstracts*, 4-8 September 2005, Ghent, Belgium, pp.91-92 (full paper to be published in *Science of the Total Environment*).

[30] Langergraber, G., Haberl, R. (2001): Constructed wetlands for water treatment. *Minerva Biotecnologica* 13(2), 123-134.

[31] Langergraber, G., Haberl, R., Laber, J., Pressl, A. (2003): Evaluation of substrate clogging processes in vertical flow constructed wetlands. *Water Science & Technology* 48(5), 25-34.

[32] Langergraber, G., Šimůnek, J. (2005): Modeling variably-saturated water flow and multi-component reactive transport in constructed wetlands. *Vadose Zone Journal* 4(4), 924-938.

[33] Lazarova, V., Manem, J. (1995): Biofilm characterisation and activity analysis in water and wastewater treatment. *Water Research* 29(10), 2227-2245.

[34] Luckner, L., Schestakow, W.M. (1991): *Migration processes in the soil and groundwater zone*. VEB, Leipzig.

[35] Mackie, R.I., Bai, R. (1993): The role of particle size distribution on the performance and modelling of filtration. *Water Science & Technology* 27(10), 19-34.

[36] Magnico, P. (2000): Impact of dynamic processes on the coupling between fluid transport and precipitate deposition. *Chem. Eng. Sci*. 55, 4323-4338.

[37] Makina, J., Wells, S.A. (2000a): A general model of the activated sludge reactor with dispersive flow – I. Model development and parameter estimation. *Water Research* 34(16), 3987-3996.

[38] Makina, J., Wells, S.A. (2000b): A general model of the activated sludge reactor with dispersive flow – II. Model verification and application. *Water Research* 34(16), 3997-4006.

[39] Martin, J.F., Reddy, K.R. (1997): Interaction and spatial distribution of wetland nitrogen processes. *Ecological Modelling* 105, 1-21.

[40] McBride, G.B., Tanner, C.C. (2000): Modelling biofilm transformations in constructed wetland mesocosms with fluctuating water level. *Ecological Engineering* 14(1-2), 93-106.

[41] Millington, R.J., Quirk. J.M. (1961): Permeability of porous solids. *Trans. Faraday Soc.* 57, 1200-1207.

[42] Molz, F.J., Widdowson, M.A., Benefield, L.D. (1986): Simulation of microbial growth dynamics coupled to nutrient and oxygen transport in porous media. *Water Resources Research* 22(8), 1207-1216.

[43] Nowak, O. (1996): Nitrifikation im Belebungsverfahren bei maßgebendem Industrieabwassereinfluß (Nitrification in the activated sludge process with significant influence of industrial wastewater). *Wiener Mitteilungen* 135, Vienna, Austria [*in German*].

[44] ÖNORM B 2505 (1997): Bepflanzte Bodenfilter (Pflanzenkläranlagen) – Anwendung, Bemessung, Bau und Betrieb (Subsurface-flow constructed wetlands – Application, dimensioning, installation and operation). Oesterreichisches Normungsinstitut, Vienna, Austria [*in German*].

[45] Padilla, F., Camara, O., Cluis, D. (1992): Modeling nitrogen species transformations and transport in the unsaturated zone considering temperature and water content effects. In: *Computer techniques and applications, Hydraulic Engineering Software IV*; Computational Mechanics Publications, Southampton, England, and Elsevier Applied Science, London, England, pp.15-26.

[46] Perfler, R., Laber, J., Langergraber, G., and Haberl R. (1999): Constructed wetlands for rehabilitation and reuse of surface waters in tropical and subtropical areas – First results from Small-Scale Plots using vertical flow beds. *Water Science & Technology* 40(3), 155-162.

[47] Pirsing, A., Wiesmann, U. (1994): Dynamische Modellierung des pH-Einflusses bei der Nitrifikation hochbelasteter Abwässer (Dynamic modelling of the pH influence in nitrification of highly concentrated wastewater). *Acta hydrochem. hydrobiol.* 22(4), 270-279.

[48] Platzer, Ch., Mauch, K. (1997): Soil clogging in vertical flow reed beds – mechanisms, parameters, consequences and ... solutions? *Water Science & Technology* 35(5), 175-181.

[49] Rassam, D., Šimůnek, J., van Genuchten, M.Th. (2003): *Modeling Variably Saturated Flow with HYDRUS-2D*. ND Consult, Brisbane, Australia, 261p, ISBN 0-646-42309-6.

[50] Rodrigo, A., Recous, S., Neel, C., Mary, B. (1997): Modelling temperature and moisture effects on C-N transformations in soils: comparison of nine models. *Ecological Modelling* 102, 325-339.

[51] Seidel, K. (1967): Über die Selbstreinigung natürlicher Gewässer. *Naturwissenschaften* 63, 286–291.

[52] Šimůnek, J., Šejna, M., van Genuchten, M.Th. (1999): The HYDRUS-2D software package for simulating the two-dimensional movement of water, heat, and multiple solutes in variably-saturated media - Version 2.0. *IGWMC - TPS - 53,* International Ground Water Modeling Center, Colorado School of Mines, Golden, Colorado, USA, 251p.

[53] Šimůnek, J., Šejna, M., van Genuchten, M.Th. (2006a): The HYDRUS Software Package for Simulating the Two- and Three-Dimensional Movement of Water, Heat, and Multiple Solutes in Variably-Saturated Media – User Manual Version 1.0. PC-Progress, Prague, Czech Republic, 160p.

[54] Šimůnek, J., van Genuchten, M.Th., Šejna, M. (2006b): The HYDRUS Software Package for Simulating the Two- and Three-Dimensional Movement of Water, Heat, and Multiple Solutes in Variably-Saturated Media – Technical Manual Version 1.0. PC-Progress, Prague, Czech Republic, 241p.

[55] Stumm, W., Morgan, J.J. (1996): *Aquatic chemistry*. 3rd edition, John Wiley & Sons, Inc., New York.

[56] Taylor, S.W., Jaffé, P.R. (1990): Biofilm growth and the related changes in the physical properties of a porous medium - 3. Dispersivity and Model Verification. *Water Resources Research* 26(9), 2171-2180.

[57] Tietz, A., Sleytr, K., Langergraber, G., Haberl, R., Kirschner, A. (2005): Characterization of microbial biocoenosis in vertical subsurface flow constructed wetlands. In: De Pauw, N., Tack,

F. (eds.): *International Symposium on "Wetland Pollutant Dynamics and Control – WETPOL" – Book of Abstracts*, 4-8 September 2005, Ghent, Belgium, pp.180-181.

[58] van Genuchten, M.Th. (1980): A closed-form equation for predicting the hydraulic conductivity of unsaturated soils. *Soil Sci. Am. J.* 44, 892-898

[59] Vandevivere, P., Baveye, P., Sanchez de Lozada, D., DeLeo, P. (1995): Microbiological clogging of saturated soils and aquifer materials: Evaluation of mathematical models. *Water Resources Research* 31(9), 2173-2180.

[60] Vanrolleghem, P.A., Spanjers, H., Petersen, B., Ginestet, P., Takács, I. (1999): Estimating (combinations of) Activated Sludge Model No.1 parameters and components by respirometry. *Water Science & Technology* 39(1), 195-214.

[61] Vymazal, J., Brix, H., Cooper, P.F., Green, M.B., Haberl, R. (eds., 1998): *Constructed wetlands for wastewater treatment in Europe*. Backhuys Publishers, Leiden, The Netherlands.

[62] Winter, K.-J., Goetz, D. (2003): The impact of sewage composition on the soil clogging phenomena of vertical flow constructed wetlands. *Water Science & Technology* 48(5), 9–14.

[63] Wood S.L., Wheeler, E.F., Berghage, R.D., Graves, R.E. (1999): Temperature effects on wastewater nitrate removal in laboratory-scale constructed wetlands. *Transactions of the ASAE* 41(1), 185-190.

[64] Yamaguchi, T., Moldrup, P., Rolston, D.E., Ito, S., Teranishi, S. (1996): Nitrification in porous media during rapid, unsaturated water flow. *Water Research* 30(3), 531-540.

[65] Zhang, T.C., Bishop, P.L. (1994): Density, porosity, and pore structure of biofilms. *Water Research* 28(11), 2267-2277.